Multiple pathways to homothallism in closely related yeast lineages in the Basidiomycota

Alexandra Cabrita[1], Márcia David-Palma[1*], Patrícia H. Brito[1], Joseph Heitman[2], Marco A. Coelho[1*] and Paula Gonçalves[1#]

[#] Corresponding author: pmz@fct.unl.pt

1. Applied Molecular Biosciences Unit-UCIBIO, Departamento de Ciências da Vida, Faculdade de Ciências e Tecnologia, Universidade Nova de Lisboa, 2829-516 Caparica, Portugal

2. Department of Molecular Genetics and Microbiology, Duke University, Duke University Medical Center, Durham, NC 27710, USA.

Running title: Homothallism in *Cystofilobasidium*

Abstract

Sexual reproduction in fungi relies on proteins with well-known functions encoded by the mating-type (*MAT*) loci. In the Basidiomycota, *MAT* loci are often bipartite, with the *P/R* locus encoding pheromone precursors and pheromone receptors and the *HD* locus encoding heterodimerizing homeodomain transcription factors (Hd1/Hd2). The interplay between different alleles of these genes within a single species usually generates at least two compatible mating types. However, a minority of species are homothallic, reproducing sexually without an obligate need for a compatible partner. Here we examine the organization and function of the *MAT* loci of *Cystofilobasidium capitatum,* a species in the order Cystofilobasidiales, which is unusually rich in homothallic species. We determined *MAT* gene content and organization in *C. capitatum* and found that it resembles a mating type of the closely related heterothallic species *Cystofilobasidium ferigula.* To explain the homothallic sexual reproduction observed in *C. capitatum* we examined HD-protein interactions in the two *Cystofilobasidium* species and determined *C. capitatum MAT* gene expression both in a natural setting and upon heterologous expression in *Phaffia rhodozyma,* a homothallic species belonging to a clade sister to *Cystofilobasidium.* We conclude that the molecular basis for homothallism in *C. capitatum* appears to be distinct from that previously established for *P. rhodozyma.* Unlike the latter species, homothallism in *C. capitatum* may involve constitutive activation or dispensability of the pheromone receptor and the functional replacement of the usual Hd1/Hd2 heterodimer by an Hd2 homodimer. Overall, our results suggest that homothallism evolved multiple times within the Cystofilobasidiales.

Importance

Sexual reproduction is important for the biology of eukaryotes because it strongly impacts the dynamics of genetic variation. In fungi, although sexual reproduction is usually associated with the fusion between

[*] Present address: Department of Molecular Genetics and Microbiology, Duke University, Duke University Medical Center, Durham, NC 27710, USA.

cells belonging to different individuals (heterothallism), sometimes a single individual is capable of completing the sexual cycle alone (homothallism). Homothallic species are unusually common in a fungal lineage named Cystofilobasidiales. Here we studied the genetic bases of homothallism in one species in this lineage, *Cystofilobasidium capitatum*, and found it to be different in several aspects when compared to another homothallic species, *Phaffia rhodozyma*, belonging to the genus most closely related to *Cystofilobasidium*. Our results strongly suggest that homothallism evolved independently in *Phaffia* and *Cystofilobasidium*, lending support to the idea that transitions between heterothallism and homothallism are not as infrequent as previously thought. Our work also helps to establish the Cystofilobasidiales as a model lineage in which to study these transitions.

Introduction

In Fungi, as in all eukaryotes, sexual reproduction is widespread, and some of the underlying mechanisms and molecular components are conserved even among distant lineages. The specific molecular pathways involved and the recognition systems responsible for triggering sexual reproduction may nonetheless vary greatly (1). Generally, sexual reproduction occurs through mating of two haploid individuals of the same species, possessing distinct mating types (2, 3). Mating types are defined by specific regions of the genome, the mating type (*MAT*) loci, which encode proteins responsible for triggering the major pathways leading to sexual development. Distinct mating types differ in the genetic content of the *MAT* loci. In basidiomycetes, mating-type determination relies on two *MAT* loci (named *P/R* and *HD*) that encode two different classes of proteins (4–6). The *HD* locus contains two divergently transcribed genes encoding homeodomain transcription factors and the *P/R* locus comprises pheromone receptor and pheromone precursor encoding genes - *STE3* and *MFA,* respectively (4, 5, 7). In the Ascomycota, only one *MAT* locus encoding transcription factors is required to determine mating-type identity. Hence, the participation of receptors and pheromones in the determination of mating type is found only in the Basidiomycota.

The *HD* and *P/R MAT* loci in Basidiomycota can be either genetically linked or unlinked in the genome of a given species. If these loci are unlinked, they may segregate independently during meiosis, leading to the generation of four distinct mating types among the haploid progeny, which is the hallmark of the tetrapolar breeding system (4, 5, 7). The bipolar breeding system results from linkage of the two *MAT* loci and yields only two mating types in the haploid progeny (4, 5, 7). Bipolar mating also takes place if one of the two (unlinked) *MAT* loci loses its function in determining mating-type identity, which has been reported occasionally for the *P/R* locus (4, 5, 7).

Although heterothallism involving the fusion between compatible mating types as a requirement for sexual reproduction is common, in some fungal species individuals are universally compatible, meaning that they can undergo sexual reproduction with any other individual, or even with or by itself, a pattern termed homothallism (3, 7, 8). In basidiomycetes few homothallic organisms have been found and even fewer have had the genetic basis of their homothallism elucidated (1, 3, 7, 8). Two relevant examples of basidiomycete yeasts with distinct molecular strategies that result in a homothallic sexual mode of reproduction are the human pathogenic yeast *Cryptococcus deneoformans* (9, 10) and *Phaffia*

77 *rhodozyma* (11). *Cryptococcus deneoformans* exhibits a particular form of homothallism named
78 unisexual reproduction, where cells of the same mating type can either fuse or undergo endoreplication
79 of the entire genome resulting in a diploid nucleus that subsequently develops into hyphae, basidia, and
80 gives rise to four haploid spores that are products of a meiotic event. Interestingly, the key genes for
81 heterothallic reproduction like *MFA*, *STE3* and even *HD1* (*SXI1)* and *HD2* (*SXI2*) appear to be
82 dispensable for unisexual reproduction of some *C. deneoformans* strains (10, 12, 13).
83 More recently, the genetic basis of homothallism was dissected in *Phaffia rhodozyma* in our
84 laboratory (11). This astaxanthin-producing basidiomycetous yeast (14) belongs to the order
85 Cystofilobasidiales, a lineage with an unusually high proportion of homothallic species (15–20), but
86 comprising also heterothallic species and others for which sexual reproduction has not yet been
87 observed. In *P. rhodozyma*, deletion mutants were used to show that the two pairs of *STE3* and *MFA*
88 genes, and the single *HD1/HD2* gene pair present in the genome, are all required for robust sexual
89 reproduction (11). The two pairs of pheromone and pheromone receptors turned out to have reciprocal
90 compatibility, a single compatible *STE3* and *MFA* pair being sufficient for sexual reproduction. This is
91 what might be expected if the *P/R* loci of two putative mating types were present in the same genome,
92 in accord with the definition of primary homothallism. The only pair of Hd1 and Hd2 proteins encoded in
93 the genome is also essential for sexual development, but the mode of action is not fully understood (11).
94 This is because Hd1 and Hd2 are usually expected to heterodimerize to form functional transcription
95 factors, but proteins encoded in the same *HD* locus do not normally form dimers. This imposes
96 heterozygosity at the *HD* locus, with dimerization occurring only between proteins encoded by different
97 gene pairs, as a condition for sexual development. In line with this, the Hd1 and Hd2 proteins of *P.*
98 *rhodozyma* that are encoded in the same gene pair, do not appear to interact strongly, leading to the
99 tentative conclusion that a weak interaction between the two proteins might suffice for function (11).
100 Therefore, the *HD* locus configuration in *P. rhodozyma* is not fully aligned with the concept of primary
101 homothallism, where the presence of two distinct pairs of *HD* genes supporting strong cross dimerization
102 between Hd1 and Hd2 proteins would be expected.
103 Here, we examine in detail the content and function of the *MAT* loci of *Cystofilobasidium*
104 *capitatum*, a homothallic species closely related to *P. rhodozyma*, in order to understand if there are
105 common features between the molecular basis of homothallism in both species. We aim to shed some
106 light on the diversity of molecular mechanisms through which homothallism can occur in the phylum
107 Basidiomycota and improve the understanding of the evolution of mating patterns in the
108 Cystofilobasidiales.
109
110
111
112 **RESULTS**
113 ***MAT* loci in *Cystofilobasidium capitatum* and *Cystofilobasidium ferigula***
114 *Cystofilobasidium capitatum* and *Cystofilobasidium ferigula* belong to the order
115 Cystofilobasidiales that also contains the genus *Phaffia*, for which two new species were recently
116 described (21), in addition to six other genera (22). The phylogenetic relationships within the order were

117 only recently clarified by a comprehensive genome-based phylogeny (21). This order contains a
118 strikingly large number of homothallic species (approximately one third of those described so far; **Table**
119 **S1 (10.6084/m9.figshare.13176422)**), a sexual mode uncommon in the Basidiomycota (3). In particular,
120 *Phaffia* is composed entirely of homothallic species (21) while *Cystofilobasidium* comprises species with
121 a variety of sexual properties, with *C. capitatum* and *C. intermedium* (23) representing the only two fully
122 homothallic species in the genus. The remaining species of *Cystofilobasidium* are heterothallic except
123 for *C. macerans*, which comprises strains exhibiting diverse sexual patterns (heterothallic, homothallic,
124 and asexual) and *C. alribaticum* for which no sexual reproduction has been observed under the
125 conditions tested (23). The genome-based phylogeny published for the Cystofilobasidiales (21) robustly
126 supported *Phaffia* and *Cystofilobasidium* as sister genera, a relationship that is recapitulated in the
127 phylogeny shown in **Fig. 1,** where a more limited number of species were included.

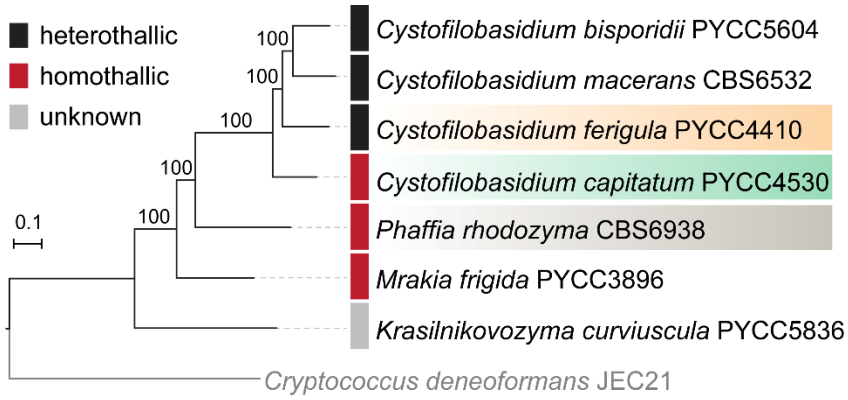

128

129 **Fig. 1.** Maximum likelihood phylogeny reconstructed from the concatenated protein alignments of 1147
130 single-copy genes shared across the studied taxa and the outgroup represented by *Cryptococcus*
131 *deneoformans*. Branch support was assessed by 1000 replicates of ultrafast bootstrap approximation
132 (UFBoot) with NNI optimization, and branch lengths are given in number of substitutions per site.
133

134 The availability of draft genomes for several *Cystofilobasidium* species allowed us to examine
135 the *MAT* loci of *C. capitatum* as well as that of the heterothallic species *C. ferigula* (**Fig. 2** and **Fig. S1**)
136 and to compare these with *MAT* loci in the homothallic *P. rhodozyma* concerning gene content and
137 organization (24). In the genome of *C. capitatum* PYCC 4530 a single pair of divergently transcribed
138 homeodomain transcription factors (*HD1* and *HD2*) was found, as well as a single pheromone receptor
139 gene (*STE3*) flanked by two identical pheromone precursor genes (*MFA1a* and *MFA1b*; **Fig 2**). These
140 two sets of genes are located on different scaffolds and encode proteins with similar lengths to their
141 counterparts in *P. rhodozyma* and the receptor is predicted to possess seven transmembrane domains
142 as expected (**Fig. 2B and Fig. S2**). Both predicted Hd proteins have homeobox domains and nuclear
143 localization signals (NLS; **Fig.S2**). However, the *MFA* genes in *C. capitatum* encode a 41 amino acid
144 pheromone precursor protein where no site for N-terminal processing could be identified (**Fig. 2C**), which
145 may compromise the formation of a mature pheromone (25). Furthermore, analysis of gene synteny
146 conservation between *Phaffia* and *C. capitatum* indicates that the *P/R* locus of *C. capitatum* may be
147 restricted to the region containing the pheromones/receptors (highlighted in yellow in **Fig. 2B**) and the

148 *HD* locus most likely includes only the *HD1* and *HD2* genes, as observed in many other basidiomycetes
149 (11, 26, 27).

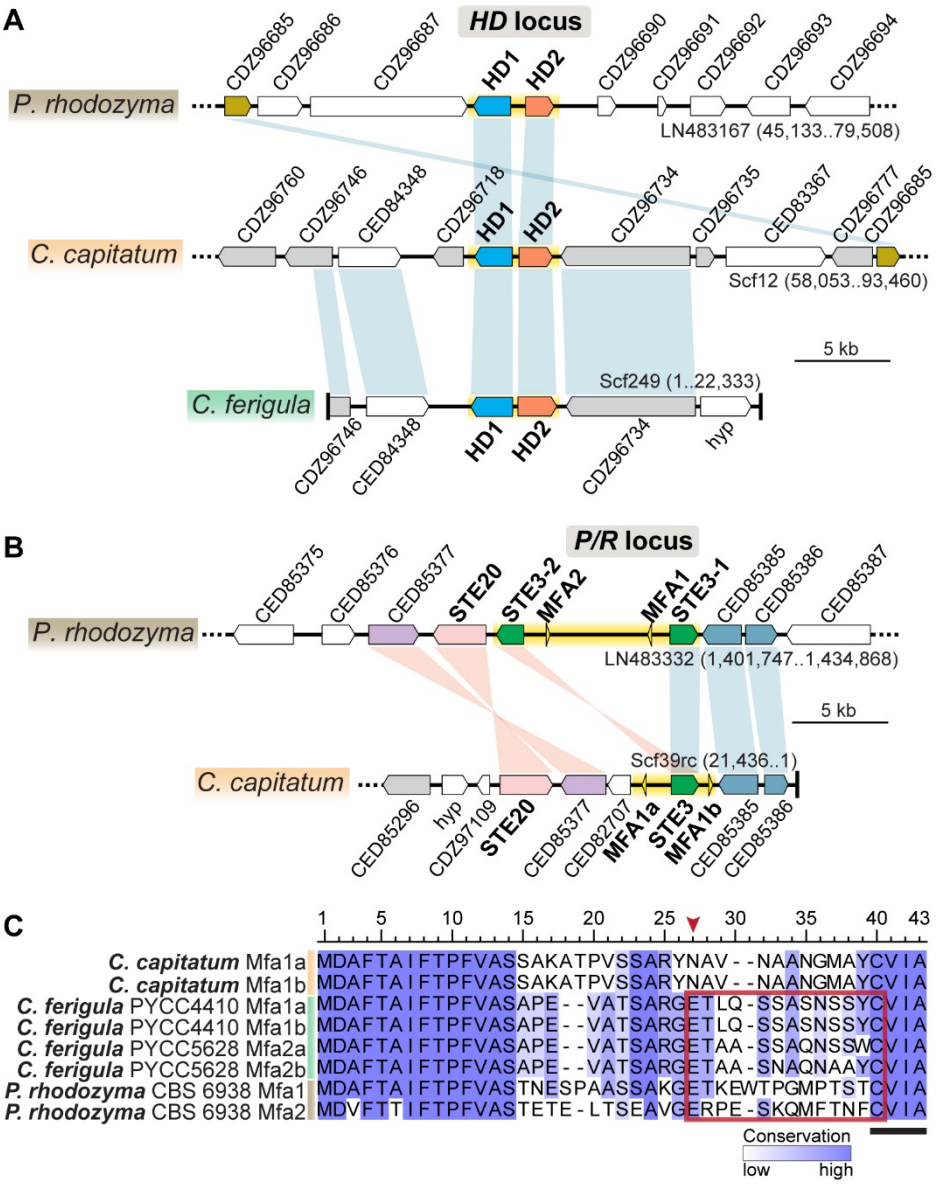

150 **Fig. 2.** Gene content and organization of the (A) *HD* and (B) *P/R* mating-type loci in *C. capitatum* and
151 *C. ferigula* (PYCC 4410), compared to *P. rhodozyma*. Genes are depicted as arrows denoting the
152 direction of transcription. The genomic regions corresponding to the putative *MAT* loci are highlighted
153 in yellow. Vertical bars connect orthologs that are in the same (blue) or inverted (pink) orientation. Non-
154 syntenic genes are shown in white, and genes in grey in *C. capitatum* and *C. ferigula* are found scattered
155 in the corresponding *P/R*- or *HD*-containing scaffold in *P. rhodozyma*, suggesting low level of synteny
156 conservation beyond the core *MAT* regions. Gene names are based on top BLASTp hits in the *P.*
157 *rhodozyma* genome and "hyp" denotes hypothetical proteins. The *P/R* locus of *C. ferigula* was omitted
158 because the available genome assemblies are too fragmented in these regions to allow for a
159 comparison. (C) Sequence alignment of pheromone precursors with amino acid positions colored in a
160 blue gradient according to conservation. Sequences proposed as the putative mature pheromones are
161 outlined by a red box, while those resembling the CAAX motif required for farnesylation are underlined.
162 In *C. capitatum* the absence of a conserved position for N-terminal processing (the two charged amino
163 acids indicated by a red arrowhead; ref 25), precludes the prediction of a mature pheromone sequence.
164

165 For *C. ferigula,* the genomes of two compatible mating types were obtained (PYCC 4410 and
166 PYCC 5628). Findings concerning *MAT* gene content were similar to *C. capitatum* (**Fig. 2** and **Fig. S1**),

and in line with the genetic composition typically found in haploid mating types of basidiomycetes. In *C. ferigula*, two genes encoding pheromone precursors were also found in each of the mating types, but in strain PYCC 5628 the two genes seem to encode slightly different mature pheromones. Because these genes are found in very small contigs in the current genome assemblies, it was not possible to determine their position in relation to the *STE3* gene nor the exact number of copies in the genome. It is conceivable that additional pheromone genes may become apparent when more complete assemblies of *C. capitatum* and *C. ferigula* genomes are available. As in *C. capitatum*, the *HD1/HD2* and the *STE3* genes were also found on different scaffolds in both *C. ferigula* strains, but the higher level of fragmentation of the current assemblies precludes a precise determination of the length and configuration of the *P/R* and *HD MAT* loci.

While heterothallic species are expected to harbour at least two different mating types with distinct alleles of *MAT* genes, this does not necessarily apply to homothallic species because there is no requirement for an operational self/nonself-recognition system in this case. To assess allele diversity of *MAT* genes in the *Cystofilobasidium* species under study, we obtained *MAT* gene sequences for as many strains as possible for both species. For *C. ferigula* two clearly distinct *STE3* alleles (sharing ~51% amino acid sequence identity) could be recognized among the five strains examined, as expected for a heterothallic species (**Fig. 3A**). For *C. capitatum,* although several different alleles could be identified in the 11 strains examined, they were much less divergent (sharing ~98% amino acid sequence identity) than *STE3* alleles known to encode proteins with different specificities, like those of *P. rhodozyma* (~50% sequence identity; (11)) and *C. ferigula* (**Fig. 3A**).

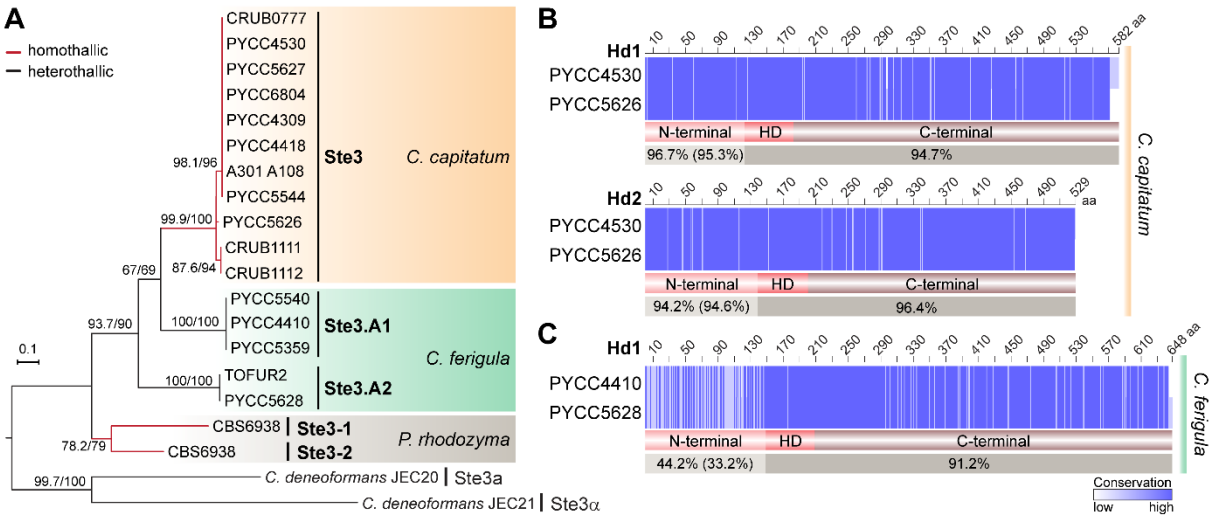

Fig. 3. Sequence diversity of *STE3* and *HD* mating-type genes in *C. capitatum* and *C. ferigula*. (A) Maximum likelihood phylogeny of pheromone receptors (Ste3) obtained from various strains of *C. capitatum* (homothallic) and *C. ferigula* (heterothallic), along with the previously characterized Ste3 sequences of *P. rhodozyma* (homothallic) and *C. deneoformans* (heterothallic). The tree was inferred with the LG+F+G4 model of amino acid substitution and was rooted in the midpoint. Branch support values separated by a slash were assessed by 10,000 replicates of both the Shimodaira-Hasegawa approximate likelihood ratio test (SH-aLRT) and the ultrafast bootstrap approximation (UFBoot). Compared to the other species, the low sequence divergence of Ste3 sequences among *C. capitatum* strains suggest the absence of functionally distinct, mating-type specific, alleles in this species. (B) and (C) Sequence alignments of the *HD1* and *HD2* gene products of *C. capitatum* and *C. ferigula*. Sequence identity between each pair of Hd1 and Hd2 proteins is given for the variable (N-termini) and conserved

200 (homeodomain and C-termini) regions with amino acid positions colored in a blue gradient according to
201 conservation. The comparison between Hd2 proteins of *C. ferigula* was not performed because the *HD2*
202 gene of PYCC 5628 is fragmented in the current genome assembly. Values in brackets for the N-
203 terminal regions are the average identity as calculated from different allele products (see **Fig. S3C** for
204 details on number of alleles). In *C. capitatum*, variable amino acid positions are evenly distributed
205 throughout the length of the Hd1 and Hd2 proteins. In contrast, the N-terminal region of Hd1 in *C. ferigula*
206 is comparatively more variable, as commonly observed in Hd1 and Hd2 proteins of other heterothallic
207 basidiomycetes (5, 7, 12, 26).
208
209 The comparison of *C. capitatum* Hd proteins suggest the existence of three main Hd variants in
210 the species with a degree of divergence between them that is lower than observed for functionally
211 different alleles of heterothallic species (**Fig. S3B and S3C)**. Moreover, for the two proteins that could
212 be examined over their entire length, the differences in the sequences are distributed homogeneously
213 throughout the protein (**Fig. 3B**), like observed for *P. rhodozyma* (11). This is unlike the divergence
214 observed in Hd1 sequences of *C. ferigula* and of other heterothallic basidiomycetes, which is more
215 extensive and concentrated in the N-terminal region responsible for self/nonself-recognition (**Fig. 3C**).
216 *C. ferigula* was reported to be bipolar, as only two different mating types had been identified so
217 far (16). This would mean that each *STE3* allele is expected to be linked to a single *HD* allele, defining
218 two mating types. However, as shown in **Fig. S3C**, our analysis uncovered three *HD* alleles, instead of
219 the expected two, and the *HD.B1* allele appears associated with the two receptors in different strains,
220 whereas the *STE3.A1* allele is associated with *HD.B1* and *HD.B3*. From these observations it seems
221 more likely that *C. ferigula* may have a tetrapolar mating system, in contrast to previous assumptions
222 (16).
223
224 **Involvement of the Hd proteins of *C. capitatum* in the homothallic sexual cycle**
225 In heterothallic basidiomycetes, the Hd1 and Hd2 proteins encoded in the *HD* locus control the
226 later stages of sexual reproduction through heterodimerization of non-allelic Hd1 and Hd2 proteins
227 brought together by cell fusion (4, 12, 26). Previous studies in our laboratory concerning the molecular
228 mechanisms of sexual reproduction of *P. rhodozyma* revealed that both the Hd1 and Hd2 proteins are
229 required for normal sporulation (which for this species consists of basidia formation), and likely act
230 through heterodimerization despite the weak nature of their interaction (11).
231 To understand if *C. capitatum* resembled *P. rhodozyma* in this respect, the yeast two-hybrid
232 assay was employed to assess the ability of the Hd1 and Hd2 proteins of *C. capitatum* to interact with
233 each other. *HD1* and *HD2* cDNAs were isolated from *C. capitatum* strain PYCC 5626 and utilized for
234 the construction of the Gal4 fusion genes for this assay. The results of the assay, presented in **Fig. 4**,
235 are consistent with a complete absence of interaction between the Hd1 and Hd2 proteins of *C.*
236 *capitatum*, unlike the results for *P. rhodozyma* (11). Notably, a strong homodimerization was detected
237 for the Hd2 protein from this species. (**Fig. 4**). Weak homodimerizations of Hd proteins were also
238 previously observed for *P. rhodozyma* (11). For *C. ferigula* a strong heterodimerization of the Hd1 and
239 Hd2 proteins derived from strains of different mating types (PYCC 5628 and PYCC 4410, respectively)
240 was noted (**Fig. 4**), in line with observations in other heterothallic basidiomycete species (12, 26).
241 Consistently, β-galactosidase activity resulting from activation of the *lacZ* reporter gene was similar to
242 the positive control both for heterodimerization of Hd proteins from *C. ferigula* and for homodimerization

of Hd2 in *C. capitatum* (**Fig. 4B**). Homodimerization of Hd1 in *C. capitatum* could not be tested, because the construct of the fusion protein between Hd1 and the Gal4 DNA binding domain could not be stably expressed in the pertinent *S. cerevisiae* strain.

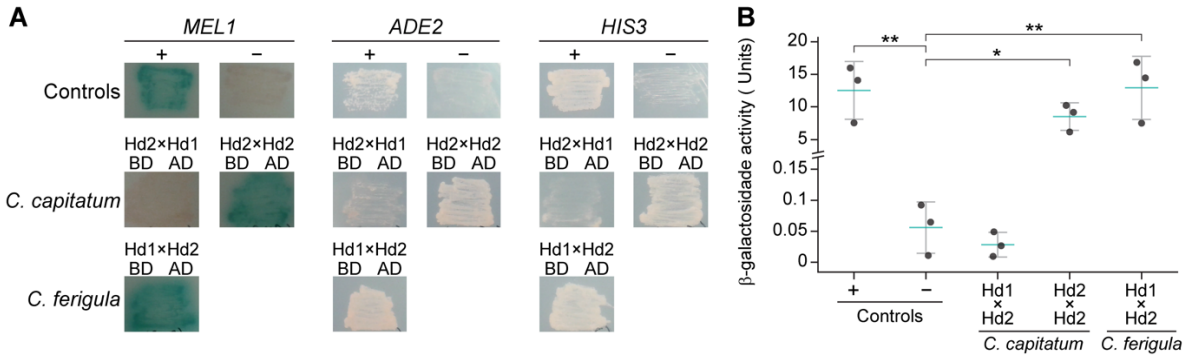

Fig. 4. Results of the Yeast Two-Hybrid assay for Hd proteins of *C. capitatum* and *C. ferigula*. (A) Qualitative results concerning the dimerization of Hd1 and Hd2 of *C. capitatum* and of *C. ferigula*, as well as homodimerization of Hd2 of *C. capitatum*, through the activation of the reporter genes *MEL1, ADE2*, and *HIS3*. Activity of the three reporter genes was tested separately in appropriate media, namely containing X-α-Gal and all required supplements *for MEL1*,or lacking supplementation with adenine (*ADE2)* or histidine *(HIS3).* Activity of the two latter reporter genes is denoted by the ability of the strains to grow on these media, while *MEL1* expression results in the formation of blue colonies. In *C. ferigula* the Hd1 protein sequence is derived from strain PYCC 5628 and the Hd2 protein is derived from strain PYCC 4410. (B) Quantitative results of the β-galactosidase assay of interactions shown in panel A. Each datapoint is the average of the activity measured in two replicate assays; the three datapoints shown for each strain represent β-galactosidase activities measured in reactions stopped after 2, 6 and 24 hours (see also Table S8 (10.6084/m9.figshare.13176422)). Blue bars denote the mean and vertical bars the standard error of the means. The interaction between a fusion protein containing the Gal4 activation domain fused to the SV40 large T-antigen and a fusion between Gal4 binding domain and p53 was used as positive control, while the negative control employed the same Gal4 activation domain fusion in combination with a fusion between Gal4 binding domain and lamin. Plasmids encoding the positive and negative control proteins were provided with the Matchmaker Gold Yeast Two-Hybrid System, by Takara Bio USA. AD, activation domain of Gal4; BD, DNA binding domain of Gal4. Significant differences between means were calculated using the Tukey's HSD test (*p<0.05, **p<0.01).

The *HD* locus of *C. capitatum* partially complements a *P. rhodozyma HD* deletion mutant

The results obtained in the yeast two-hybrid assay suggest that homodimerization of Hd2 may play a role in homothallic sexual development in *C. capitatum,* possibly functionally replacing the usual Hd1/Hd2 heterodimer. To investigate this, we set out to assess function of the *C. capitatum HD* locus by heterologous expression in a *P. rhodozyma HDΔ* mutant.

Integration of the complete *HD* locus of *C. capitatum* strain PYCC 4530 in the rDNA locus of the *P. rhodozyma HDΔ* mutant (construct *HDΔ+HD1/HD2-PYCC4530*) resulted in a very weak but consistent recovery of sporulation (**Table 1, Table S2 and Table S3 (10.6084/m9.figshare.13176422)**). Because no interaction between the Hd1 and Hd2 proteins could be detected in the yeast two-hybrid assay but instead strong homodimerization of the Hd2 protein was observed, we subsequently decided to assess whether expression of *HD2* alone was sufficient to restore sexual development of the *P. rhodozyma HDΔ* mutant. To this end, a construct containing in addition to the intergenic region only a residual (344 bp) 5´portion of the *HD1* gene (excluding the homeodomain; *HDΔ+HD2-PYCC4530*) was used to transform the *P. rhodozyma HDΔ* mutant. In this mutant that expresses only the Hd2 protein,

284 sporulation levels like those observed upon transformation of the complete *C. capitatum HD* locus were
285 observed (**Table 1, Table S2 and Table S3 (10.6084/m9.figshare.13176422)**), suggesting that only the
286 Hd2 protein is required for the observed complementation.
287
288
289 **Table 1.** Complementation of *P. rhodozyma MAT* loci mutant strains with *C. capitatum* genes.
290 Sporulation (basidia formation) patterns were scored qualitatively using the criteria explained as given
291 in the key.
292

Strain	*P. rhodozyma* WT	*HD*Δ	*HD*Δ*+HD2-PYCC4530*	*HD*Δ*+HD1/HD2-PYCC4530*	*P/R*Δ	*P/R*Δ*+STE3/MFA-PYCC4530*
Sporulation* phenotype	+++*	–	+	+	–	–

293
294 *Basidia counted on the surface of 30 colonies per assay; results were scored from two to four essays per strain;
295 (–): < 5 basidia; (+): 5-30 basidia; (+++) > 1000 basidia.
296
297
298 **The *HD1 and HD2* genes of *C. capitatum* are differently expressed during growth in sporulation**
299 **conditions and in *P. rhodozyma* mutants**
300 To substantiate the hypothesis that Hd2 might be the sole important component in the *HD* locus
301 of *C. capitatum*, we compared the expression levels of *HD1* and *HD2* in *C. capitatum* PYCC 5626, in
302 sporulation conditions, and in the *P. rhodozyma* mutant containing the complete *HD* locus of *C.*
303 *capitatum* PYCC 4530 (construct *HD*Δ*+HD1/HD2-PYCC4530*). The results, depicted in **Fig. 5**, show
304 that of the *HD* gene pair, only the *HD2* gene seems to be substantially expressed in the *C. capitatum*
305 strain. Heterologous expression of *HD2* in the *P. rhodozyma* mutant, although much lower than in *C.*
306 *capitatum*, can be easily detected, while heterologous expression of *HD1* seems to be only vestigial.
307

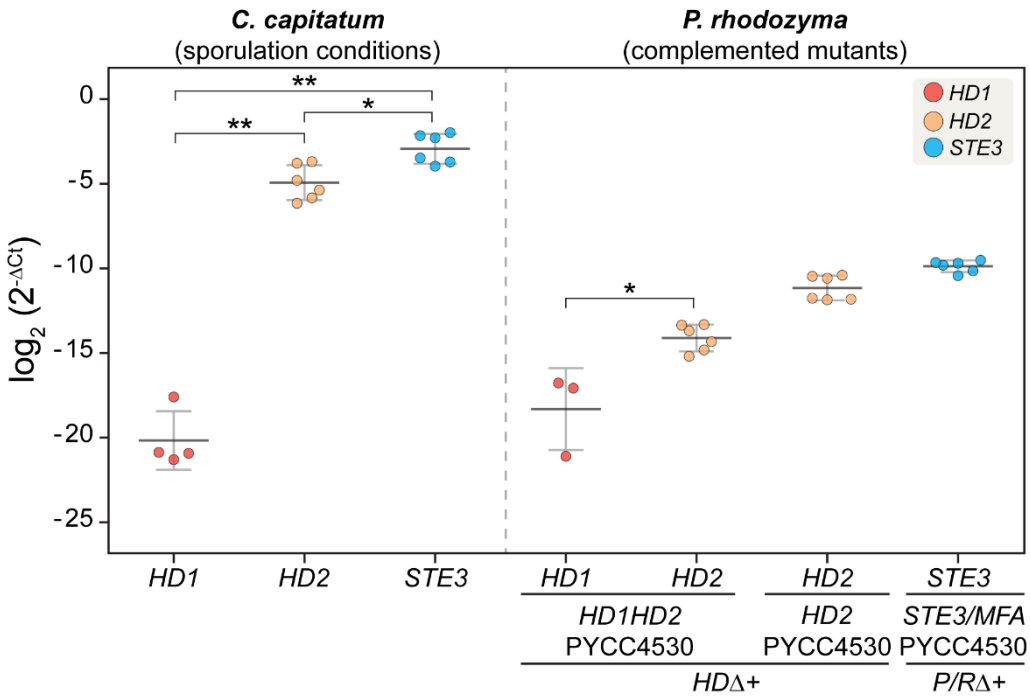

Fig. 5. Real time quantitative PCR results of *MAT* gene expression in *C. capitatum* under sporulation conditions and in *P. rhodozyma* complemented mutants. Expression of *MAT* genes is given as $\log_2$ fold difference relative to the expression of actin in each strain. These results are derived from two biological replicates, each assayed in triplicate, resulting in six datapoints for each measurement. For *HD1* expression assays less than six dots are plotted because in some reactions *HD1* expression was undetectable. Significant differences between the expression of different genes were calculated with the Mann-Whitney test (*p<0.05, **p<0.01).

P/R locus of *C. capitatum* does not restore sporulation in a *P. rhodozyma* cognate deletion mutant

Because Hd function could be assessed using heterologous expression, a *P. rhodozyma* deletion mutant of both *P/R* clusters (*P/RΔ*) was similarly used as host for the *P/R* locus of *C. capitatum* strain PYCC 4530, encompassing the *STE3* and *MFA1*a genes and the respective native promotor regions (*P/RΔ+STE3/MFA-PYCC4530*). However, integration of the *P/R* locus of *C. capitatum* in the rDNA of the *P. rhodozyma P/RΔ* mutant failed to restore sporulation (**Table 1 and Table S2 (10.6084/m9.figshare.13176422)**), although the *C. capitatum STE3* gene was expressed in *P. rhodozyma* (**Fig. 5**). Interestingly, *STE3* is the most expressed among *MAT* genes of *C. capitatum* PYCC 5626 (**Fig. 5**), suggesting it may have a role in sexual reproduction despite our inability to observe it in the heterologous setting.

DISCUSSION

The main aim of this study was to ascertain to which extent common features could be found between the molecular bases of homothallism in different species of the Cystofilobasidiales, a lineage in the Basidiomycota particularly rich in species exhibiting this uncommon sexual behaviour. The molecular basis of homothallism was previously dissected in the genetically tractable Cystofilobasidiales

335 species *P. rhodozyma* (11). Here, we characterized the *MAT* loci of a second homothallic species
336 belonging to a sister genus, *C. capitatum,* by examining the structure of the loci in the available genome
337 of strain PYCC 4530 and by comparing *MAT* gene sequences in a total of 11 *C. capitatum* strains. The
338 most striking difference between the *MAT* loci in *P. rhodozyma* and *C. capitatum* is the presence in the
339 latter species of a single pheromone receptor gene, instead of the two distinct and functionally
340 complementary sets of pheromone receptor and pheromone precursor genes found in *P. rhodozyma*.
341 Therefore, the *C. capitatum MAT* gene content resembles a haploid mating type of a heterothallic
342 species (4), while that of *P. rhodozyma* is reminiscent of a fusion between two mating types (11).
343 However, like in *P. rhodozyma*, no evidence for functionally distinct variants (alleles) of *MAT* genes that
344 might form different mating types were found in *C. capitatum,* consistent with its homothallic behaviour.
345 We subsequently devised various experimental approaches to try to bring to light functional features of
346 *MAT* genes in *C. capitatum.* In these experimental approaches two *C. capitatum* strains were used: in
347 addition to sequenced strain PYCC 4530, strain PYCC 5626 was employed for the isolation of cDNAs
348 because unlike other strains, it readily sporulates in different experimental conditions.
349 *P. rhodozyma* can be described as a primary homothallic basidiomycete, with reciprocal
350 compatibility between the pheromones and receptors of the two *P/R* clusters and with a weak
351 heterodimerization between the only pair of Hd1 and Hd2 proteins being responsible for triggering of its
352 sexual cycle, with possible hints at homodimerization events (11). Therefore, in *P. rhodozyma*, the *P/R*
353 system seems to work similarly to what might be expected for a heterothallic mating type, while the *HD*
354 locus is apparently operating through weak dimerization between adjacently encoded Hd1 and Hd2.
355 This dimerization normally occurs only between proteins encoded by different *HD* alleles. Hence, the
356 weak interaction in *P. rhodozyma* may have evolved to support sexual development in the absence of
357 a second *HD* allele. Because the *MAT* loci in *C. capitatum* have the same gene content as haploid
358 mating types of heterothallic species, in this case both the *P/R* and the *HD* loci probably underwent
359 changes in their mode of operation to permit homothallism. For the *HD* locus, the complete absence of
360 interaction between the Hd1 and Hd2 proteins, the formation of Hd2 homodimers, complementation
361 results of the *P. rhodozyma HD⊿* mutant and the very low expression of the *HD1* gene suggest that the
362 *HD* locus is relevant for sporulation but also that regulatory functions normally fulfilled by the Hd1/Hd2
363 heterodimer may have been taken over by the Hd2 homodimer. Hd1 homodimerization was not tested
364 due to technical difficulties. Although it would have been very interesting to be able to test also Hd1
365 homodimerization, this lost importance when gene expression experiments showed that *HD1*
366 expression was barely detectable. Interestingly, the α2 transcription factor, which is the Hd1 *S.*
367 *cerevisiae* homologue, is capable of forming both a homodimer that represses transcription of **a**-specific
368 genes in haploid α-cells, and a heterodimer with the a1 transcription factor (Hd2 homologue) that
369 represses haploid-specific genes in diploid cells (28). This suggests that these proteins can operate
370 both as homodimers and as heterodimers. However, to our knowledge, functional Hd1 or Hd2
371 homodimers have not been reported so far in basidiomycetes, although there was some evidence for
372 homodimerization of Hd proteins in *P. rhodozyma* (11). Our hypothesis for the mode of action of the
373 *HD* locus predicts that Hd1 might be dispensable. In some heterothallic basidiomycetes, it has been
374 shown that the Hd1 and Hd2 proteins hold different functional domains that are essential for function of

375 the transcription regulation complex (29–31). One such species is the mushroom *Coprinopsis cinerea*,
376 where it has been shown that Hd1 contributes with the NLS region, allowing the heterodimer to be
377 transported into the nucleus, while the homeodomain of Hd2 is required for binding of the complex to
378 DNA (29, 32). Hence, in this case, formation of a heterodimer is required for function. In *C. capitatum*,
379 Hd2 possesses both an NLS and a homeodomain so in that perspective it seems possible that Hd2 may
380 indeed play a role in the homothallic life cycle of *C. capitatum* that is sufficient and independent of Hd1.
381 It is possible that this hypothesized function of Hd2 evolved recently in this species, which could explain
382 the fact that the *HD1* is not pseudogenized. Alternatively, the Hd1 may have acquired a function
383 unrelated to sexual reproduction, which might entail its expression under different conditions, and justify
384 its maintenance in the genome. Despite multiple attempts, the methods used to transform *P. rhodozyma*
385 failed to yield transformants of *C. capitatum,* which precluded the possibility of testing the hypothesis
386 regarding the role of Hd2 in this species by deletion of the *HD2* gene.
387 Introduction of the *P/R* locus into the *P. rhodozyma P/R*Δ mutant failed to restore sporulation of
388 the cognate mutant, even though expression of the *STE3* gene in the heterologous setting could be
389 demonstrated. The explanations for this are presently unclear, since the ability of Ste3-like receptors to
390 activate heterologously a sexual development pathway over a much larger phylogenetic distance was
391 previously demonstrated (33). As to the mode of action of the receptor in its normal setting, the possibility
392 that it could be constitutively active should be considered, in line with the fact that the predicted
393 pheromone precursor genes lack the N-terminal processing signals, likely precluding the formation of
394 an active pheromone. Mutations within the pheromone receptor that can lead to constitutively active
395 receptors have been previously reported, resulting in a bypass of the pheromone for sexual reproduction
396 (25, 33–36). Mutations in the pheromone that allow it to activate the receptor encoded in the same *P/R*
397 cluster are also known (25, 37). In fact, mutations that lead to self-activation or self-compatibility have
398 been proposed to form the basis for the transition from a tetrapolar to a bipolar mating system, or even
399 from a heterothallic to a homothallic mating behaviour (3, 5) for some species. If the pheromone system
400 does not operate normally in *C. capitatum*, this may be a reason for the lack of complementation of the
401 *P. rhodozyma P/R*Δ mutant by the *C. capitatum P/R* locus.
402 Hence, taken together, our results suggest that *P. rhodozyma* and *C. capitatum* attained
403 homothallic breeding systems through different mechanisms, which is consistent with the hypothesis
404 that the *P. rhodozyma* mating system arose at the origin of the genus, possibly by fusion of *P/R* loci of
405 compatible mating types and the adaptation of the HD dimerization system. *C. capitatum*, on the other
406 hand, has an extant makeup of its *MAT* loci that suggests it may have evolved from a heterothallic
407 mating type, in which the Hd2 homodimer acquired a prominent role. If a mature pheromone is formed
408 despite the absence of an N-terminal processing signal, it might be that the pheromone-receptor pair in
409 *C. capitatum* have become self-activating. On the other hand, if no mature pheromone is formed, the
410 pheromone receptor gene might have bypassed the pheromone requirement and is now constitutively
411 active. Whatever the case may be, the *P/R* system still likely has a role in some aspects of the sexual
412 development, which in agreement with the fact that *STE3* gene seems to be highly expressed. Although
413 we cannot discard the hypothesis that the receptor is fulfilling a role unrelated to sexual reproduction,

414 and while such receptors have been reported (38), they were not associated with pheromone precursor
415 genes.
416 The different particularities of homothallism in the two Cystofilobasidiales species studied so far
417 are suggestive of remarkable levels of plasticity in the evolution of sexual reproduction in this order. It
418 will be interesting to conduct similar studies in other homothallic species of this order, which would allow
419 us to get a more complete insight in the array of mechanisms involved as well as possible genomic
420 rearrangement that may have been involved in the transitions between heterothallic and homothallic
421 species. Having uncovered *P. rhodozyma* as a viable host for heterologous expression, opens the
422 possibility of assessing the functionality of other *MAT* proteins from uncharacterised species in this
423 order.
424
425 **MATERIALS AND METHODS**
426 **Strains and culture conditions**
427 *P. rhodozyma*, *C. capitatum* and *C. ferigula* strains (**Table S4**
428 **(10.6084/m9.figshare.13176422)**) were routinely grown in YPD medium (2% Peptone, 1% Yeast
429 Extract, 2% Glucose, 2% Agar) at 17 to 20ºC. For the preparation of electrocompetent cells, *P.*
430 *rhodozyma* strains were grown in YPD liquid medium at 20ºC, and transformants were incubated at
431 17ºC in selective medium, consisting of YPD plates supplemented with the appropriate antifungal drugs
432 (100 µg/ml of geneticin and/or 100 µg/ml of zeocin and/or 100 µg/ml of hygromycin B).
433 *Escherichia coli* strain DH5α (Gibco-BRL, Carlsbad, CA, USA) was used as a cloning host and
434 was grown at 37ºC in LB medium (1% NaCl, 1% Tryptone, 0.5% Yeast Extract and 2% Agar for solid
435 medium) supplemented with ampicillin at 100 µg/ml when appropriate.
436
437 **DNA extraction, genome sequencing and assembly**
438 Genomic DNA of *C. ferigula* PYCC 5628 was extracted from single cell-derived cultures using
439 the ZR Fungal/Bacterial DNA MiniPrep kit (ZYMO Research). DNA samples were quantified using Qubit
440 2.0. Genome sequencing was carried out by commercial providers, at the Genomics Unit of Instituto
441 Gulbenkian de Ciência, and at the Sequencing and Genomic Technologies Core Facility of the Duke
442 Center for Genomic and Computational Biology. Two short insert-size libraries (~500 bp) were prepared
443 with the Nextera Kit and subsequently sequenced using the Illumina MiSeq and HiSeq2500 systems to
444 generate paired 300- and 151-nt reads, respectively. After adaptor clipping using Trimmomatic (v0.36)
445 the two sets of reads were assembled with SPAdes (v3.11.1) (39) (with parameters: "--careful" to reduce
446 the number of mismatches and short indels in the final assembly, and the k-mer sizes: 21, 33, 55, 77,
447 99, 127, automatically selected based on read length). Genome assembly quality was assessed by the
448 QUAST (v.5.0.2) (40), and gene models were predicted ab initio using Augustus (41) trained on
449 *Cryptococcus neoformans*. Genome sequencing data generated, and final genome assembly statistics
450 are given in **Table S5 (10.6084/m9.figshare.13176422)**.
451
452 **Identification of mating-type genes and synteny analyses**

453 Scaffolds containing *MAT* genes, namely the homeodomain transcription factors (*HD1*/*HD2*)
454 and the mating pheromones (*MFA*) and receptors (*STE3*), were identified by BLASTP or TBLASTN in
455 the genome assemblies of *C. capitatum* PYCC 4530 (=CBS 7420; BioProject: PRJNA371774) and *C.*
456 *ferigula* PYCC 4410 (BioProject: PRJNA371786), and in the newly obtained assembly of *C. ferigula*
457 PYCC 5628 (BioProject: PRJNA371793). Well-annotated *P. rhodozyma MAT* proteins (11) were used
458 as search query. The retrieved *MAT* genes were manually reannotated if required and analysed further:
459 (i) the transmembrane regions in the pheromone receptor protein were predicted by HMMTOP software
460 (42); (ii) the Homeodomain regions in Hd1 and Hd2 proteins were predicted by InterPro server (43) and
461 compared to the previously characterized homeodomain proteins in Pfam database; (iii) nuclear
462 localization signals (NLS) and coiled-coil motifs were identified in the complete Hd1 and Hd2 sequences
463 using, respectively, the SeqNLS (with a 0.8 cut-off) (44) and Jpred4 (45) (see **Figs. S1B** and **S1C** and
464 **Fig. S2**). Synteny between *MAT* regions of different strains and species was based on bidirectional
465 BLAST analyses of the corresponding predicted proteins. The short pheromone precursor genes in the
466 genomes of *C. ferigula* and *C. capitatum* were identified manually as they usually fail automatic
467 detection.
468
469 **Species and MAT gene phylogenies**
470 A phylogenetic analysis representing major lineages within Cystofilobasidiales was inferred on
471 a concatenated protein dataset of single copy core genes of four *Cystofilobasidium* species, *Phaffia*
472 *rhodozyma* CBS 6938, *Mrakia frigida* PYCC 3896, *Krasilnikovozyma curviuscula* PYCC 5836, and the
473 outgroup *Cryptococcus deneoformans* JEC21 (**Table S**4 (10.6084/m9.figshare.13176422)).
474 Orthologous clusters were inferred with all-against-all BLASTP (NCBI Blast-2.2) searches and the
475 Markov cluster algorithm (OrthoMCL v1.4; (46)) with inflation factor (F) of 1.5, and minimum pairwise
476 sequence alignment coverage of 50% implemented in GET_HOMOLOGUES package (47). Clusters
477 present in single copy in all analyzed genomes were retained, aligned with MAFFT v7.407 using the G-
478 INS-I method and default parameter values (48), trimmed with BMGE v1.12 using the amino acid option
479 (49), and finally concatenated into a single data set. The species phylogeny was inferred with IQ-TREE
480 v1.6.12 (50) using maximum-likelihood (ML) inference under a LG+F+I+G4 model of sequence
481 evolution. ModelFinder (51) was used to determine best-fit model according to Bayesian Information
482 Criterion (BIC) and branch support was estimated using ultrafast bootstrap approximation (UFBoot) with
483 NNI optimization (52), both implemented in IQ-TREE package.
484 To analyse the *MAT* gene content across strains of *C. capitatum* and *C. ferigula*, protein
485 sequences of the *HD1*, *HD2* and *STE3* genes were retrieved from the genome assemblies and aligned
486 separately. Conserved regions were used to design primers to amplify the corresponding genomic
487 regions across the available strains of each species (**Table S6 (10.6084/m9.figshare.13176422)**).
488 These regions include a ~ 870-bp region of the *STE3* gene, and a ~1.5-kb fragment encompassing the
489 5′ end and intergenic regions of the *HD1* and *HD2* genes (**Table S6 (10.6084/m9.figshare.13176422)**
490 **and Fig. S3**). Genomic DNA was extracted through a standard Phenol-Chloroform method (53) and the
491 regions of interest were PCR-amplified, purified using Illustra GFX PCR DNA and Gel Band Purification
492 Kit (GE Healthcare Life Sciences), and then sequenced by Sanger Sequencing, at STABVida (Portugal).

493 For phylogenetic analysis of *MAT* genes, amino acid or nucleotide sequences were individually aligned
494 with MAFFT v7.310 (48) using the L-INS-i strategy (--localpair --maxiterate 1000) and poorly aligned
495 regions were trimmed with TrimAl (--gappyout) (54). The resulting alignments were input to IQ-TREE
496 v.1.6.5 (50) ML phylogenies using best-fit models automatically determined by ModelFinder (51)
497 (parameter: -m MFP). The exact model employed in tree reconstruction is given in the respective figure
498 legends. Branch support values were obtained from 10,000 replicates of both UFBoot (52) and the
499 nonparametric variant of the approximate likelihood ratio test (SH-aLRT) (55). In addition, the option "-
500 bnni" was employed to minimize the risk of overestimating branch supports with UFBoot when in
501 presence of severe model violations. The resulting phylogenies were midpoint rooted and graphically
502 visualized with iTOL v5.5.1 (56).
503
504
505 **Yeast Two-Hybrid assay**
506 To assess the interaction between the Hd1 and Hd2 proteins, the Matchmaker Gold Yeast Two-
507 Hybrid System kit (Takara) was used. In this system, fusion proteins containing the Gal4 DNA binding
508 domain (BD) are expressed from plasmid pGBKT7 in *MAT***a** haploid strain Y2HGold, while fusion
509 proteins containing the Gal4 activation domain (AD) are expressed from plasmid pGADT7 in *MAT***α**
510 haploid strain Y187. Diploid strains expressing both AD and BD fusion proteins are used to test
511 interactions and are obtained by mating the haploid strains expressing each of the fusion proteins of
512 interest. Hence, coding DNA sequences of the pertinent *HD* genes were cloned into pGADT7 and
513 pGBKT7, so as to yield plasmids expressing the desired fusion proteins.
514 Synthetic genes designed using the coding DNA sequences of the *HD1* and *HD2* genes of *C.*
515 *ferigula* and were synthesised at Eurofins Genomics (Germany). The *HD1* and *HD2* gene sequences of
516 strains PYCC 4410 and PYCC 5628 from *C. ferigula* respectively were adapted to the *S. cerevisiae*
517 codon usage (**Fig. S4**). The synthetic genes were obtained as inserts of pEX-A258 plasmids.
518 cDNAs of *HD1* and *HD2* from *C. capitatum* were obtained from total RNA isolated from strain PYCC
519 5626, briefly as follows. Strain PYCC 5626 was cultivated in GSA medium (0.2% Glucose, 0.2%
520 Soytone) in 10% of the flask volume, for 8 days at 20ºC and 90 rpm (Sartorius Certomat IS incubator),
521 until inspection under the microscope revealed the presence of teliospores (16). RNA extraction was
522 performed using the *ZR Fungal/Bacterial RNA MiniPrep kit* (by ZYMO Research), with a single step of
523 in-column DNase I Digestion to free the RNA samples of genomic DNA. cDNA was synthesized from
524 total mRNA using Maxima H Minus Reverse Transcriptase (by Thermo Scientific) and oligo (dT)20 as
525 primer, and synthesis of the second DNA strand was performed using specific primers for the complete
526 *HD1* and *HD2* genes (**Table S6 (10.6084/m9.figshare.13176422)**). The fragments corresponding to the
527 *HD1* and *HD2* cDNA sequences of strain PYCC 5626 were sequenced by Sanger Sequencing, at
528 STABVida (Portugal). The protein sequences of Hd1 and Hd2 of strain PYCC 5626 were aligned with
529 those of strain PYCC 4530 (**Fig. 3.B**) using the software MUSCLE (implemented in the software Unipro
530 UGENE v1.30.0 (57)) and the level of intraspecific variability was calculated.
531 The *HD1* and *HD2* complete synthetic genes from *C. ferigula* and cDNA fragments from *C.*
532 *capitatum* were amplified using primers that contained 40 bp tails at their 5' ends that correspond to the

533 flanking regions of the Multiple Cloning Sites present in pGADT7 and in pGBKT7 (**Table S6**
534 **(10.6084/m9.figshare.13176422)**). Plasmid pGADT7 was then linearized at the Multiple Cloning Site
535 by digestion with Cla I (Thermo Scientific), while pGBKT7 was linearized by digestion with Pst I (Thermo
536 Scientific). *S. cerevisiae* strains Y187 and Y2HGold were transformed with inserts and linearized vectors
537 using the transformation method described in the Yeastmaker Yeast Transformation System 2 protocol.
538 Transformants were selected in appropriate media (Yeast Nitrogen Base without amino acids, with
539 appropriate supplements (**Table S7 (10.6084/m9.figshare.13176422)**)) at 30ºC. Transformantions with
540 linearized pGBKT7 and the *C.capitatum* Hd1 insert resulted in numbers of transformants similar to those
541 observed in other transformations. However, unlike in other transformations, all transformants
542 investigated harboured plasmids without insert. This was observed only for this combination of vector
543 and insert and persisted in different transformation attempts.
544 Mating of haploid *S. cerevisiae* strains was performed by incubating a single colony from each
545 of the two haploid transformants to be mated in 200 µl of YPD medium at 30ºC, for 24 hours, at 250
546 rpm. After incubation, the cells were recovered and thoroughly washed with distilled sterile water and
547 plated on appropriate selective media (**Table S7 (10.6084/m9.figshare.13176422)**).
548 In the Matchmaker Gold Yeast Two-Hybrid System the *MEL1, ADE2 and HIS3* reporter genes
549 are used for qualitative assessment of interactions using plate assays, while the *LacZ* reporter gene is
550 used only to quantify the strength of the interaction, through quantification of β-galactosidase activity in
551 cell extracts. To test the activation of the *ADE2* and *HIS3* reporter genes, diploid strains were plated on
552 appropriate selective media without adenine or histidine, respectively, while to test the activation of the
553 yeast *MEL1* reporter gene encoding a secreted α–galactosidase, haploid transformants (to check for
554 autoactivation; Fig. S5) and diploid derivatives were plated on appropriate selective medium
555 supplemented with X-α-Gal (Takara Bio) at a final concentration of 40 µg/ml.
556 To quantify activation of the *LacZ* reporter gene, a β-galactosidase activity assay was performed, using
557 o-nitrophenyl β-D-galactopyranoside (ONPG) as a substrate. The assay was performed as described in
558 the Yeast Protocols Handbook (Takara Bio). All reactions were performed in triplicate, so that they could
559 be stopped at 3 different points in time (after 2 hours, 6 hours, and 24 hours), by the addition of 0.4 mL
560 of 1M Na_2CO_3 to each suspension. Raw data concerning these assays is shown in **Table S8**
561 **(10.6084/m9.figshare.13176422).**
562
563 **Construction of recombinant plasmids and gene deletion cassettes**
564 For the construction of *P. rhodozyma* mutants, recombinant plasmids and gene deletion
565 cassettes were constructed, as follows. Primer sequences (**Table S6 (10.6084/m9.figshare.13176422)**)
566 were based on available genome sequences of *P. rhodozyma* strain CBS 6938 (NCBI project
567 PRJEB6925 (58)) and *C. capitatum* strain PYCC 4530 (Bioproject PRJNA371774). Plasmids used for
568 the constructions were pJET1.2/blunt (Thermo Scientific), pPR2TN containing a geneticin resistance
569 cassette (59) and pBS-HYG (60) containing a hygromycin resistance cassette. All fragments used for
570 cloning and deletion cassettes were amplified by PCR using Phusion High-Fidelity DNA polymerase
571 (Thermo Scientific) and the amplified products were purified using either *Illustra GFX PCR DNA and Gel*

572 *Band Purification Kit* (GE Healthcare) or *GeneJET Gel Extraction Kit* (Thermo Scientific). Constructions
573 were performed using standard molecular cloning methods (61) and *E. coli* strain DH5α as host.
574
575 **Transformation of *P. rhodozyma***
576 *P. rhodozyma* strains (CBS 6938 and mutants) (**Table S4 (10.6084/m9.figshare.13176422)**)
577 were transformed by electroporation, with the linearized recombinant plasmids or deletion cassettes, as
578 previously described by Visser *et al*, 2005 (62), reducing the amount of DNA used to 2 μg for the
579 transformations of the complemented *P. rhodozyma* mutants. The electroporation conditions (Gene
580 Pulser II Electroporation System, Bio-Rad) consisted of an internal resistance of 1000 Ω, an electric
581 pulse of 0.8 kV, a capacitance of 25 μF, resulting in a pulse ranging from 18 to 20 ms (63, 64). The cells
582 recovered subsequently in YPD liquid medium, for at least 2.5 hours at 17 ºC before being plated on
583 YPD medium supplemented with the appropriate antifungal drug and incubated at 17ºC. The genotypes
584 of the transformants were determined as previously described (11, 65).
585
586 ***P. rhodozyma* sporulation (basidia formation) assays**
587 To determine the ability of the *P. rhodozyma* mutants to sporulate, basidia formation assays
588 were performed, where the strains were incubated in DWR solid medium with 0.5% of ribitol (0.5%
589 Ribitol and 2.5% Agar), as previously described (11). Each basidia formation assay was conducted on
590 3 plates containing DWR+0.5% ribitol. On each plate, 10 colonies of each strain to be tested were
591 spotted. Different strains were employed in each assay as indicated in **Table S2**
592 **(10.6084/m9.figshare.13176422)**, but in all assays the *P. rhodozyma* wild type was used as a positive
593 control. Colonies were examined under the microscope using 100x magnification after 10 and 20 days
594 of incubation at 18ºC, and basidia formation patterns were scored qualitatively. The numbers of basidia
595 counted in experiment E8 for the complemented mutants concerning the study of the *HD* locus of *C.*
596 *capitatum* after 20 days of incubation are listed in **Table S3 (10.6084/m9.figshare.13176422)**. In all
597 cases the entire colony was submitted to microscopic observation.
598
599 **Real-time quantitative PCR to assess expression of the *MAT* genes**
600 Total RNA was extracted from a sporulating culture of *C. capitatum* strain PYCC 5626.
601 Sporulation (teliospore formation in the case of this species) was induced by incubation in GSA liquid
602 medium (0.2% Glucose, 0.2% Soytone) in 10% the volume of the flask, at 17ºC, without agitation, until
603 microscopic inspection revealed hyphae and teliospores, the latter being thick-walled resting spores
604 from which basidia arise (16). Total RNA extraction was performed using the *ZR Fungal/Bacterial RNA*
605 *MiniPrep kit* (by ZYMO Research). *P. rhodozyma* complemented mutants were grown in YPD liquid
606 medium to an OD_{600nm} of 1.0. The cultures were then collected and frozen at -80ºC for 1 hour before
607 proceeding with total RNA extraction through a standard Trizol method. In-column DNase I digestion to
608 free the RNA samples of genomic DNA using the RNA Clean & Concentrator kit (by ZYMO Research)
609 was used for all samples, and absence of gDNA was verified by PCR. cDNA was synthesized from total
610 mRNA using Maxima H Minus Reverse Transcriptase (Thermo Scientific) and oligo (dT)20 as primer.
611 Real-Time PCR was performed using the SensiFAST SYBR No-ROX kit (by Bioline, London), with 20μl

612 reactions, in a Rotor-Gene 6000 Corbett apparatus. The reaction parameters consisted of an initial
613 denaturation step at 95ºC, for 2 min, followed by 40 cycles of 95ºC for 5 seconds, 57ºC for 10 seconds
614 and 72ºC for 20 seconds. Two biological replicates were performed, with triplicates performed for each
615 reaction (**Table S9 (10.6084/m9.figshare.13176422)**). Relative expression of the *MAT* genes was
616 calculated using the $2^{-\Delta Ct}$ method, where $\Delta Ct = Ct_{test} - Ct_{reference}$, as described by Livak and Schmittgen
617 (66), and expression values were represented as the $\log_2 (2^{-\Delta Ct})$. Mann-Whitney tests were performed
618 to determine if the differences in expression of genes within each strain were statistically different.
619
620 **Data availability**
621
622 Nucleotide sequences been deposited in NCBI/EMBL (GenBank) under accession numbers:
623 MT561333-MT561342 (*C. capitatum STE3*); MT561330-MT561332 (*C. ferigula STE3*); MT592882-
624 MT592890 and MT592891-MT592894 (respectively for *C. capitatum* and *C. ferigula* 5'-end and
625 intergenic region of *HD1* and *HD2*). Sequencing reads for *C. ferigula* PYCC 5628 (BioProject
626 PRJNA371793) are available in the NCBI SRA database. The *C. ferigula* PYCC 5628 draft genome
627 assembly has been deposited at DDBJ/ENA/GenBank under accession numbers MVAN00000000.
628
629
630 **ACKNOWLEDGEMENTS**
631 The authors are very thankful to Alex Idnurm, Brenda Wingfield, Timothy James, and Paul Dyer for
632 their insightful and thorough reviews of this manuscript. This work was supported by UCIBIO-Unidade
633 de Ciências Biomoleculares Aplicadas, which is financed by Portuguese funds from Fundação para a
634 Ciência e Tecnologia, Ministério da Ciência, Tecnologia e Ensino Superior (FCT/MCTES;
635 https://www.fct. pt/) grant UID/Multi/04378/2019 and FCT/MCTES grants PTDC/BIA-
636 GEN/112799/2009 (to P.G.), SFRH/BPD/79198/2011 (M.C.) and SFRH/BD/81895/2011 (M.D.P.). This
637 work also benefited from the support of the INCD computing infrastructure funded by FCT and FEDER
638 under the project 01/SAICT/2016 nº 022153. This work was also supported by NIH/NIAID R37 Award
639 AI39115-23 and R01 award AI50113-16. J.H. is co-director and fellow for CIFAR program Fungal
640 Kingdom: Threats & Opportunities.

641

642

643 **References**

644 1. Lee SC, Ni M, Li W, Shertz C, Heitman J. 2010. The evolution of sex: a perspective from
645 the fungal kingdom. Microbiol Mol Biol Rev 74:298–340.
646 2. Stanton BC, Hull CM. 2007. Mating-Type Locus Control of Cell Identity, p. 59–73. *In*
647 Heitman, J, Kronstad, JW, Taylor, JW, Casselton, LA (eds.), Sex in fungi: molecular
648 determination and evolutionary implications. ASM Press, Washington, DC.

649 3. Lin X, Heitman J. 2007. Mechanisms of homothallism in fungi and transitions between
650 heterothallism and homothallism, p. 35–57. *In* Heitman, J, Kronstad, JW, Taylor, JW,
651 Casselton, LA (eds.), Sex in fungi: molecular determination and evolutionary
652 implications. ASM Press, Washington, D.C.
653 4. Coelho MA, Bakkeren G, Sun S, Hood ME, Giraud T. 2017. Fungal sex: the
654 Basidiomycota. Microbiol Spectr 5:FUNK-0046-2016.
655 5. Fraser JA, Hsueh Y-P, Findley KM, Heitman J. 2007. evolution of the mating-type locus:
656 the Basidiomycetes, p. 19–34. *In* Heitman, J, Kronstad, JW, Taylor, JW, Casselton, LA
657 (eds.), Sex in Fungi: Molecular Determination and Evolutionary Implications. ASM
658 Press, Washington, DC.
659 6. Raudaskoski M, Kothe E. 2010. Basidiomycete mating type genes and pheromone
660 signaling. Eukaryot Cell 9:847–859.
661 7. Kües U, James TY, Heitman J. 2011. Mating type in basidiomycetes: unipolar, bipolar,
662 and tetrapolar patterns of sexuality, p. 97–160. *In* Pöggeler, S, Wöstemeyer, J (eds.),
663 The Mycota, Evolution of Fungi and Fungal-Like Organisms, Volume XIV. Springer,
664 Berlin Heidelberg.
665 8. Wilson AM, Wilken PM, van der Nest MA, Steenkamp ET, Wingfield MJ, Wingfield BD.
666 2015. Homothallism: an umbrella term for describing diverse sexual behaviours. IMA
667 Fungus 6:207–214.
668 9. Lin X, Hull CM, Heitman J. 2005. Sexual reproduction between partners of the same
669 mating type in *Cryptococcus Neoformans*. Nature 434:1017–1021.
670 10. Wang L, Lin X. 2011. Mechanisms of unisexual mating in *Cryptococcus neoformans*.
671 Fungal Genet Biol 48:651-660.
672 11. David-Palma M, Sampaio JP, Gonçalves P. 2016. Genetic dissection of sexual
673 reproduction in a primary homothallic basidiomycete. PLoS Genet 12: e1006110.
674 12. Hull CM, Boily M, Heitman J. 2005. Sex-specific homeodomain proteins sxi1 α and sxi2
675 a coordinately regulate sexual development in *Cryptococcus neoformans*. Eukaryot
676 Cell 4:526–535.
677 13. Gyawali R, Zhao Y, Lin J, Fan Y, Xu X, Upadhyay S, Lin X. 2017. Pheromone independent
678 unisexual development in *Cryptococcus neoformans*. PLOS Genet 13:e1006772.
679 14. Barredo J, García-Estrada C, Kosalkova K, Barreiro C. 2017. Biosynthesis of astaxanthin
680 as a main carotenoid in the heterobasidiomycetous yeast *Xanthophyllomyces*

681 *dendrorhous*. J Fungi 3:44.
682 15. Kurtzman CP, Fell JW, Boekhout T. 2011. The Yeasts, a Taxonomic Study, 5th ed.
683 Elsevier.
684 16. Sampaio JP. 2011. *Cystofilobasidium* Oberwinkler & Bandoni (1983), p. 1423–1432. *In*
685 Kurtzman, CP, Fell, JW, Boekhout, T (eds.), The Yeasts, a Taxonomic Study, 5th ed.
686 Elsevier.
687 17. Fell JW, Johnson EA, Scorzetti G. 2011. *Xanthophyllomyces* Golubev (1995), p. 1595–
688 1599. *In* Kurtzman, CP, Fell, JW, Boekhout, T (eds.), The Yeasts, a Taxonomic Study,
689 5th ed. Elsevier.
690 18. Fell JW. 2011. *Mrakia* Y. Yamada & Komagata (1987), p. 1503–1510. *In* Kurtzman, CP,
691 Fell, JW, Boekhout, T (eds.), The Yeasts, a Taxonomic Study, 5th ed. Elsevier.
692 19. Sampaio JP. 2011. *Tausonia* Bab'eva (1998), p. 1999–2001. *In* Kurtzman, CP, Fell, JW,
693 Boekhout, T (eds.), The Yeasts, a Taxonomic Study, 5th ed. Elsevier.
694 20. Takashima M, Nakase T. 2011. *Udeniomyces* Nakase & Takematsu (1992), p. 2063–
695 2068. *In* Kurtzman, CP, Fell, JW, Boekhout, T (eds.), The Yeasts, a Taxonomic Study,
696 5th ed. Elsevier.
697 21. David-Palma M, Libkind D, Brito PH, Silva M, Bellora N, Coelho MA, Heitman J,
698 Gonçalves P, Sampaio JP. 2020. The untapped australasian diversity of astaxanthin-
699 producing yeasts with biotechnological potential - *Phaffia australis* sp. nov. and
700 *Phaffia tasmanica* sp. nov. Microorganisms 8, 1651.
701 22. Kachalkin A V, Turchetti B, Inácio J, Carvalho C, Mašínová T, Pontes A, Röhl O,
702 Glushakova AM, Akulov A, Baldrian P, Begerow D, Buzzini P, Sampaio JP, Yurkov AM.
703 2019. rare and undersampled dimorphic basidiomycetes. Mycol Prog 18:945–971.
704 23. Pontes A, Röhl O, Carvalho C, Maldonado C, Yurkov AM, Paulo Sampaio J. 2016.
705 *Cystofilobasidium intermedium* sp. nov. and *Cystofilobasidium alribaticum* f.a. sp.
706 nov., isolated from mediterranean forest soils. Int J Syst Evol Microbiol 66:1058–1062.
707 24. Bellora N, Moliné M, David-Palma M, Coelho MA, Hittinger CT, Sampaio JP, Gonçalves
708 P, Libkind D. 2016. Comparative genomics provides new insights into the diversity,
709 physiology, and sexuality of the only industrially exploited tremellomycete: *Phaffia*
710 *rhodozyma*. BMC Genomics 17:901.
711 25. Kües U. 2015. From two to many: multiple mating types in basidiomycetes. Fungal Biol
712 Rev 29:126–166.

713 26. Kämper J, Reichmann M, Romeis T, Bölker M, Kahmann R. 1995. multiallelic
714 recognition: nonself-dependent dimerization of the bE and bW homeodomain
715 proteins in *Ustilago maydis*. Cell 81:73–83.
716 27. Maia TM, Lopes ST, Almeida JMGCF, Rosa LH, Sampaio JP, Gonçalves P, Coelho MA.
717 2015. evolution of mating systems in basidiomycetes and the genetic architecture
718 underlying mating-type determination in the yeast *Leucosporidium scottii*. Genetics
719 201:75–89.
720 28. Dranginis AM. 1990. Binding of yeast a1 and α2 as a heterodimer to the operator dna
721 of a haploid-specific gene. Nature 347:682–685.
722 29. Asante-Owusu RN, Banham AH, Böhnert HU, Mellor EJC, Casselton LA. 1996.
723 heterodimerization between two classes of homeodomain proteins in the mushroom
724 *Coprinus cinereus* brings together potential dna-binding and activation domains. Gene
725 172:25–31.
726 30. Schlesinger R, Kahmann R, Kämper J. 1997. The homeodomains of the heterodimeric
727 Be And Bw proteins of *Ustilago maydis* are both critical for function. Mol Gen Genet
728 254:514–519.
729 31. Van Diepen LTA, Olson A, Ihrmark K, Stenlid J, James TY. 2013. Extensive trans-specific
730 polymorphism at the mating type locus of the root decay fungus *Heterobasidion*. Mol
731 Biol Evol 30:2286–2301.
732 32. Kües U, Göttgens B, Stratmann R, Richardson W V, O'Shea SF, Casselton L a. 1994. A
733 chimeric homeodomain protein causes self-compatibility and constitutive sexual
734 development in the mushroom *Coprinus cinereus*. EMBO J 13:4054–4059.
735 33. Hsueh Y-P, Xue C, Heitman J. 2009. A constitutively active GPCR governs morphogenic
736 transitions in *Cryptococcus neoformans*. EMBO J 28:1220–1233.
737 34. Olesnicky NS, Brown AJ, Dowell SJ, Casselton LA. 1999. A constitutively active G-
738 protein-coupled receptor causes mating self-compatibility in the mushroom *Coprinus*.
739 EMBO J 18:2756–2763.
740 35. Boone C, Davis NG, Sprague GF. 1993. Mutations that alter the third cytoplasmic loop
741 of the a-factor receptor lead to a constitutive and hypersensitive phenotype. Proc Natl
742 Acad Sci 90:9921–9925.
743 36. Fowler TJ, Mitton MF, Vaillancourt LJ, Raper CA. 2001. changes in mate recognition
744 through alterations of pheromones and receptors in the multisexual mushroom

745 fungus *Schizophyllum commune*. Genetics 158:1491–1503.
746 37. Riquelme M, Challen MP, Casselton LA, Brown AJ. 2005. The origin of multiple *b*
747 mating specificities in *Coprinus cinereus*. Genetics 170:1105–1119.
748 38. Díaz-Valderrama JR, Aime MC. 2016. The cacao pathogen *Moniliophthora roreri*
749 (Marasmiaceae) possesses biallelic *A* and *B* mating loci but reproduces clonally.
750 Heredity 116:491–501.
751 39. Bankevich A, Nurk S, Antipov D, Gurevich AA, Dvorkin M, Kulikov AS, Lesin VM,
752 Nikolenko SI, Pham S, Prjibelski AD, Pyshkin A V, Sirotkin A V, Vyahhi N, Tesler G,
753 Alekseyev MA, Pevzner PA. 2012. SPAdes: a new genome assembly algorithm and its
754 applications to single-cell sequencing. J Comput Biol 19:455–477.
755 40. Mikheenko A, Prjibelski A, Saveliev V, Antipov D, Gurevich A. 2018. Versatile genome
756 assembly evaluation with QUAST-LG. Bioinformatics 34:i142–i150.
757 41. Stanke M, Diekhans M, Baertsch R, Haussler D. 2008. Using native and syntenically
758 mapped cDNA alignments to improve *de novo* gene finding. Bioinformatics 24:637–
759 644.
760 42. Tusnády GE, Simon I. 2001. The HMMTOP transmembrane topology prediction server.
761 Bioinformatics 17:849–850.
762 43. Mitchell A, Chang H, Daugherty L, Fraser M, Hunter S, Lopez R, McAnulla C,
763 McMenamin C, Nuka G, Pesseat S, Sangrador-Vegas A, Scheremetjew M, Rato C, Yong
764 S, Bateman A, Punta M, Attwood T, Sigrist C, Redaschi N, Rivoire C, Xenarios I, Kahn D,
765 Guyot D, Bork P, Letunic I, Gough J, Oates M, Haft D, Huang H, Natale D, Wu C, Orengo
766 C, Sillitoe I, Mi H, Thomas P, Finn R. 2015. The InterPro protein families database: the
767 classification resource after 15 years. Nucleic Acids Res 43:D213-221.
768 44. Lin J rong, Hu J. 2013. SeqNLS: nuclear localization signal prediction based on frequent
769 pattern mining and linear motif scoring. PLoS One 8:e76864.
770 45. Drozdetskiy A, Cole C, Procter J, Barton GJ. 2015. JPred4: a protein secondary
771 structure prediction server. Nucleic Acids Res 43:W389–W394.
772 46. Li L, Stoeckert Jr CJ, Roos DS. 2003. OrthoMCL: identification of ortholog groups for
773 eukaryotic genomes. Genome Res 13:2178–2189.
774 47. Contreras-Moreira B, Vinuesa P. 2013. GET_HOMOLOGUES, a versatile software
775 package for scalable and robust microbial pangenome analysis. Appl Environ Microbiol
776 79:7696–7701.

777 48. Katoh K, Standley DM. 2013. MAFFT Multiple Sequence Alignment Software Version 7:
778 Improvements in Performance and Usability. Mol Biol Evol 30:772–780.
779 49. Criscuolo A, Gribaldo S. 2010. BMGE (Block Mapping and Gathering with Entropy): a
780 new software for selection of phylogenetic informative regions from multiple
781 sequence alignments. BMC Evol Biol 10:210.
782 50. Nguyen L-T, Schmidt HA, von Haeseler A, Minh BQ. 2015. IQ-TREE: a fast and effective
783 stochastic algorithm for estimating maximum-likelihood phylogenies. Mol Biol Evol
784 32:268–274.
785 51. Kalyaanamoorthy S, Minh BQ, Wong TKF, von Haeseler A, Jermiin LS. 2017.
786 ModelFinder: fast model selection for accurate phylogenetic estimates. Nat Methods
787 14:587–589.
788 52. Hoang DT, Chernomor O, von Haeseler A, Minh BQ, Vinh LS. 2018. UFBoot2:
789 Improving the Ultrafast Bootstrap Approximation. Mol Biol Evol 35:518–522.
790 53. Gonçalves P, Valério E, Correia C, de Almeida JMGCF, Sampaio JP. 2011. Evidence for
791 divergent evolution of growth temperature preference in sympatric *Saccharomyces*
792 species. PLoS One 6:e20739.
793 54. Capella-Gutiérrez S, Silla-Martínez JM, Gabaldón T. 2009. trimAl: A tool for automated
794 alignment trimming in large-scale phylogenetic analyses. Bioinformatics 25:1972–
795 1973.
796 55. Guindon S, Dufayard JF, Lefort V, Anisimova M, Hordijk W, Gascuel O. 2010. New
797 algorithms and methods to estimate maximum-likelihood phylogenies: Assessing the
798 performance of PhyML 3.0. Syst Biol 59:307–321.
799 56. Letunic I, Bork P. 2019. Interactive Tree Of Life (iTOL) v4: recent updates and new
800 developments. Nucleic Acids Res 47:W256–W259.
801 57. Okonechnikov K, Golosova O, Fursov M, Varlamov A, Vaskin Y, Efremov I, German
802 Grehov OG, Kandrov D, Rasputin K, Syabro M, Tleukenov T. 2012. Unipro UGENE: A
803 unified bioinformatics toolkit. Bioinformatics 28:1166–1167.
804 58. Sharma R, Gassel S, Steiger S, Xia X, Bauer R, Sandmann G, Thines M. 2015. The
805 genome of the basal agaricomycete *Xanthophyllomyces dendrorhous* provides insights
806 into the organization of its acetyl-CoA derived pathways and the evolution of
807 Agaricomycotina. BMC Genomics 16:233.
808 59. Verdoes JC, Krubasik P, Sandmann G, Van Ooyen AJJ. 1999. Isolation and functional

809 characterisation of a novel type of carotenoid biosynthetic gene from
810 *Xanthophyllomyces dendrorhous*. Mol Gen Genet 262:453-461.
811 60. Niklitschek M, Alcaíno J, Barahona S, Sepúlveda D, Lozano C, Carmona M, Marcoleta
812 A, Martínez C, Lodato P, Baeza M, Cifuentes V. 2008. Genomic organization of the
813 structural genes controlling the astaxanthin biosynthesis pathway of
814 *Xanthophyllomyces dendrorhous*. Biol Res 41:93-108.
815 61. Sambrook J, Russell D. 2001. Molecular Cloning: A Laboratory Manual, 3rd ed. Cold
816 Spring Harbor Laboratory Press, New York.
817 62. Visser H, Sandmann G, Verdoes JC. 2005. Xanthophylls in Fungi. Metabolic engineering
818 of the astaxanthin biosynthetic pathway in *Xanthophyllomyces dendrorhous.*
819 Microbial Processes and Products.pp 257-272.
820 63. Rodríguez-Sáiz M, Godio RP, Álvarez V, De La Fuente JL, Martín JF, Barredo JL. 2009.
821 The NADP-dependent glutamate dehydrogenase gene from the astaxanthin producer
822 *Xanthophyllomyces dendrorhous*: Use of its promoter for controlled gene expression.
823 Mol Biotechnol 41:165-172.
824 64. Wery J, Verdoes JC, Van Ooyen AJJ. 1998. Efficient transformation of the astaxanthin-
825 producing yeast *Phaffia rhodozyma*. Biotechnol Tech 12:399-405.
826 65. Lin G, Bultman J, Johnson EA, Fell JW. 2012. Genetic manipulation of
827 *Xanthophyllomyces dendrorhous* and *Phaffia rhodozyma*. Methods Mol Biol 898:235–
828 249.
829 66. Livak KJ, Schmittgen TD. 2001. Analysis of relative gene expression data using real-
830 time quantitative PCR and the 2-ΔΔCT method. Methods 25:402–408.
831
832
833
834
835
836
837
838
839
840
841
842

Supplementary Figures

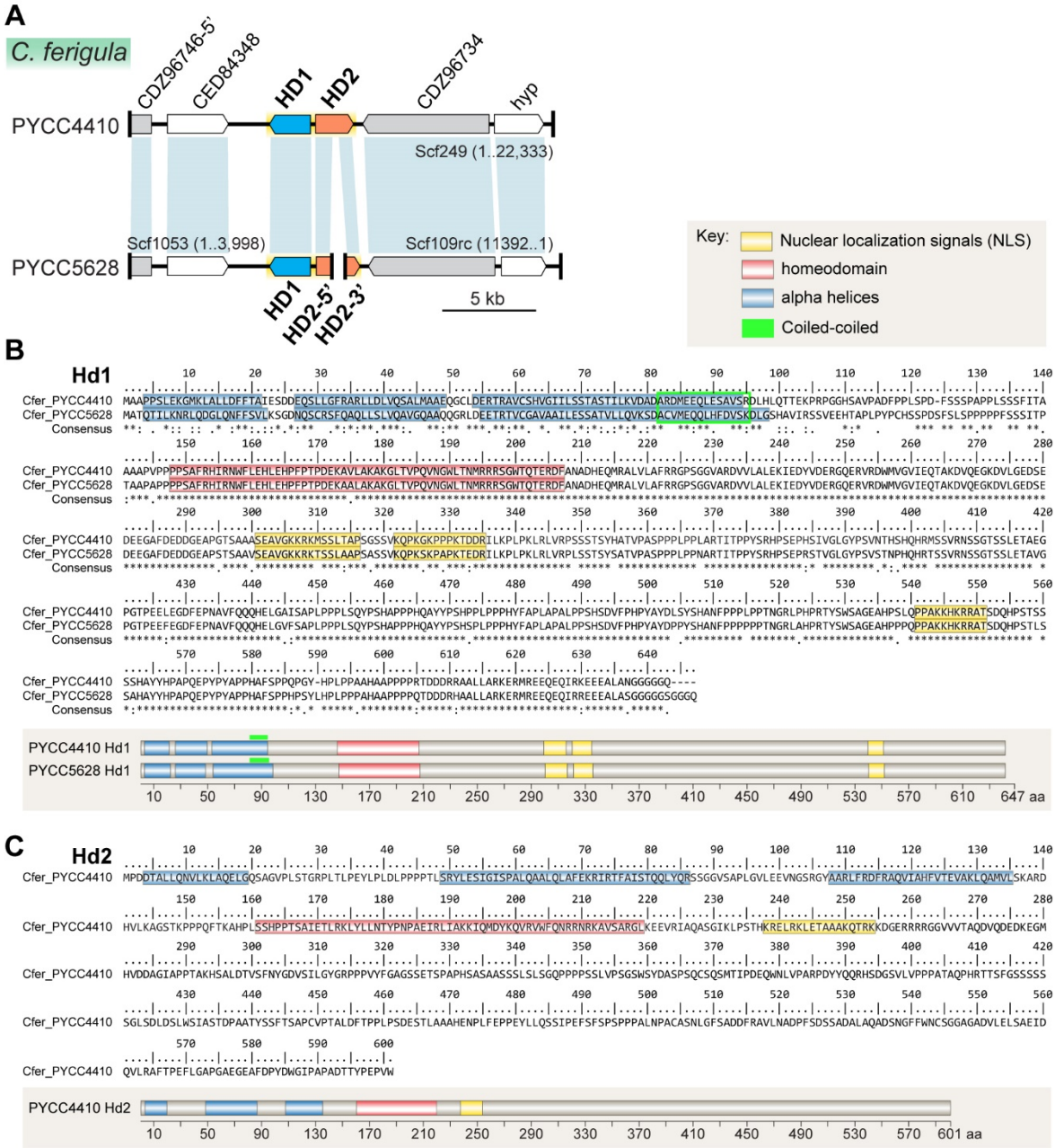

Fig. S1. Analysis of the *HD* locus of *C. ferigula*. (A) Genomic organization of the *HD1* and *HD2* genes in *C. ferigula* PYCC 4410 and PYCC 5628. The *HD2* gene in strain PYCC 5628 is fragmented and localizes, as depicted, at the ends of two different scaffolds. However, comparative analysis indicates this region is syntenic in both *C. ferigula* strains. (B) Hd1 amino acid sequences of strains PYCC 4410 and PYCC 5628 shown as a sequence alignment (on the top) and as a schematic representation (on the bottom). (C) Hd2 amino acid sequence of *C. ferigula* PYCC 4410. In panels B and C, typical protein secondary structure features are highlighted according to the key on the top right.

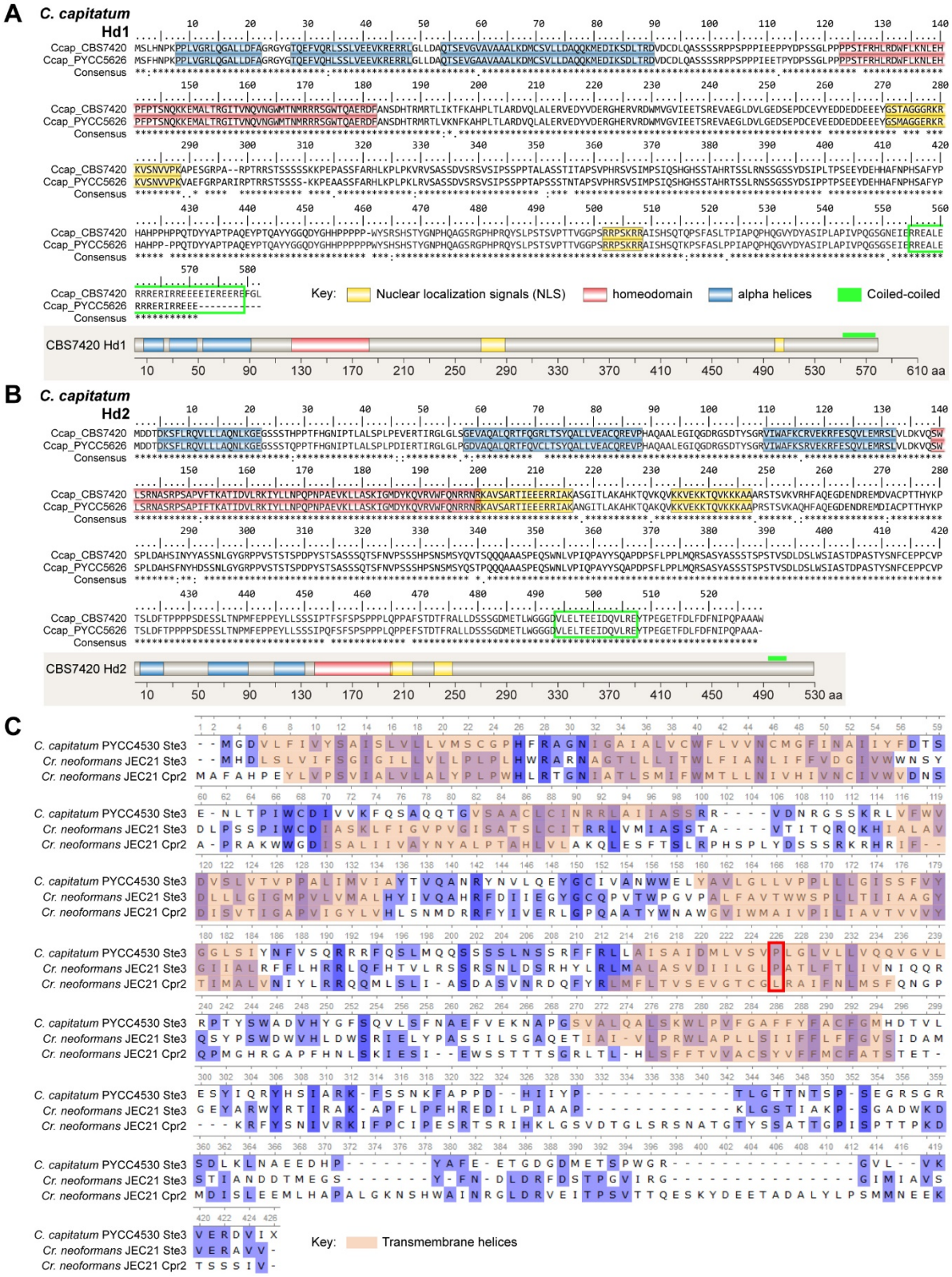

Fig. S2. Sequence alignment of the (A) *HD1* and (B) *HD2* gene products from *C. capitatum* PYCC 4530 and PYCC 5626. In both panels, the amino acid sequence alignment is shown on the top and a schematic representation is shown below. Typical protein secondary structure features are highlighted according to the key on the bottom.(C) Sequence alignment of the Ste3 receptors from *C. capitatum* and *C. neoformans,* and the *C. deneoformans* pheromone receptor-like Cpr2*,* highlighting the seven transmembrane domains. The constitutive activity of Cpr2 in *C. deneoformans* results from an

unconventional residue, Leu[222], in place of a conserved proline in transmembrane domain six (red box; Hsueh Y-P, Xue C, and Heitman J, EMBO J 28:1220–1233, 2009).

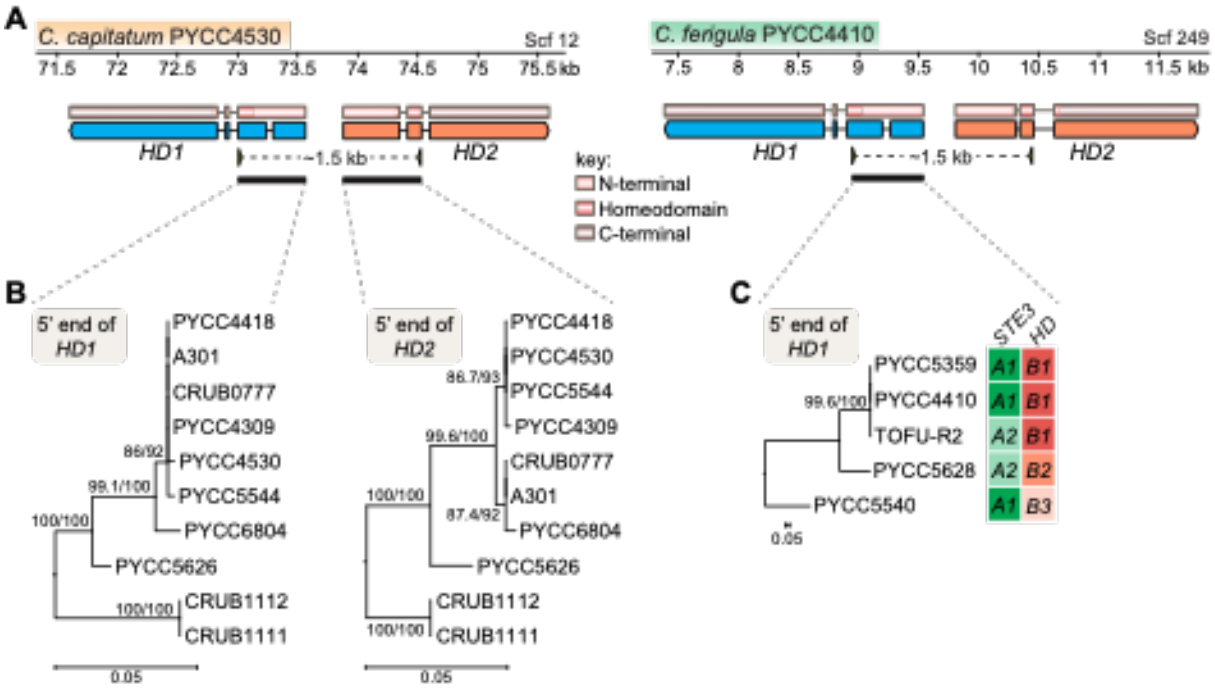

Fig. S3.

Fig. S3. Determination of different alleles of the *HD* loci in *C. capitatum* and *C. ferigula*. (A) A ~1.5-kb-long genomic region spanning the homeodomain, the 5' end region, and the common intergenic region of the *HD1* and *HD2* genes was PCR-amplified and sequenced from available 10 strains of *C. capitatum* and 5 strains of *C. ferigula*. Primers locations are shown as yellow arrowheads below the genes. (B) Maximum likelihood phylogenies inferred from the 5' end of the *HD1* and *HD2* genes (regions underlined in panel A) of *C. capitatum* using the best-fit substitution models HKY+F and K2P, respectively. (C) Maximum likelihood phylogeny inferred from the 5' end of the *HD1* gene of *C. ferigula* using the best-fit model K2P. Note that the branch length in the two *HD1* gene trees is quite different (scale bars in nucleotide substitutions per site), which implies a much higher divergence of the *C. ferigula HD1* alleles compared to the *HD1* alleles of *C. capitatum*. The trees are rooted in the midpoint and branch support values separated by a slash were assessed by 10,000 replicates of both Shimodaira-Hasegawa approximate likelihood ratio test (SH-aLRT) and the ultrafast bootstrap approximation (UFBoot). The molecular mating type assigned for each of the analyzed strains of *C. ferigula* provides evidence that this species has a biallelic *P/R* locus and a multiallelic *HD* locus, which are genetically unlinked (the *B1* allele appears associated with both *A1* and *A2* alleles).

***C. ferigula* PYCC5628 *HD1* synthetic gene sequence**

```
   1 ATGGCAACCCAAACTATTCTCAAAAACCGACTTCAGGACGGGCTGCAGAATTTCTTCAGTGTACTAAAAAGCGGTGACAACCAGTCATGTCGAAGTTTCC
 101 AGGCACAACTTCTTTCACTAGTCCAGGCTGTTGGACAAGCAGCACAGCAGGGGCGGTTGGATGAGGAAACCAGAACGGTATGTGGTGCTGTAGCAGCCAT
 201 ACTTGAATCGAGCGCCACTGTCCTTCTTCAGGTTAAGTCTGACGCCTGTGTTATGGAACAGCAGCTGCATTTTGATGTTAGCAAAGATCTAGGCTCGCAT
 301 GCCGTGATAAGGTCGTCCGTGGAAGAACACACGGCGCCATTGCCCTACCCTTGCCACTCCTCGCCTGACTCGTTTAGTTTAAGCCCACCGCCCCCGCCAT
 401 TCTCCTCTAGCATCACACCAACGGCGGCACCCGCTCCGCCTCCACCATCTGCTTTTCGCCACATCAGAAACTGGTTTTTGGAGCATCTGGAACACCCGTT
 501 CCCTACACCTGACGAAAAAGCCGCGTTAGCCAAAGCAAAAGGTTTAACTGTTCCACAAGTTAACGGTTGGCTAACAAATATGAGGCGCAGGTCGGGTTGG
 601 ACTCAAACAGAAAGGGATTTCGCCAACGCAGATCATGAACAAATGAGAGCGCTCGTGCTAGCCTTTCGGAGAGGCCCTTCCGGTGGCGTAGCCAGAGATG
 701 TCGTGTTGGCCCTAGAAAAAATAGAAGACTATGTGGATGAAAGGGGACAAGAAAGAGTCAGAGATTGGATGGTAGGTGTGATCGAGCAAACCGCTAAAGA
 801 CGTACAAGAAGGAAAGGACGTTCTGGGTGAGGATTCCGAGGATGAAGAAGGAGCATTTGATGAGGATGACGGAGAAGCGCCCAGTACGAGTGCGGCCGTC
 901 AGCGAAGCTGTGGGGAAGAAACGTAAAACAAGTTCTTTGGCTGCACCATCCGCCAGCTCAGTCAAACAACCTAAATCTAAACCAGCGCCAAAGACTGAAG
1001 ATCGTATTCTGAAGCCGTTGCCGAAGTTGAGGCTCGTAAGGCCTTTGTCATCAACTAGTTACTCTGCAACTGTTCCCGCCAGTCCGCCACCATTGCCCCC
1101 AAATGCGAGGACCATTACCCCGCCCTACAGTCGTCACCCAAGTGAGCCTAGAAGTACTGTTGGCTTGGGGTACCCATCTGTTTCAACTAATCCTCATCAA
1201 CATAGAACCTCTTCTGTCAGAAATTCATCAGGAACATCATCACTAGAAACCGCCGTTGGACCGGGAACTCCGGAAGAATTCGAAGGCGACTTCGAGCCAA
1301 ATGCTGTTTTTCAACAACAACATGAGTTAGGCGTTTTTTCAGCTCCCTTACCGCCTCCTTTGTCCCAATACCCCTCTCACGCCCCCCCCCCCCATCAAGC
1401 ATATTACCCTTCCCACTCACCATTGCCTCCCCCCCACTACTTTGCTCCTTTGGCTCCCGCATTACCACCTTCCCATTCCGATGTTTTTCCTCACCCATAC
1501 GCATATGATCCACCTTATTCCCACGCTAATTTTCCACCACCTCCTCCACCAACTAATGGCCGTTTAGCACACCCTCGTACATATTCTTGGTCAGCTGGTG
1601 AAGCTCATCCTCCACCACAACCACCAGCTAAGAAGCATAAGAGAAGAGCTACATCTGATCAACATCCTTCTACATTATCATCTGCACATGCTTATTATCA
1701 TCCAGCACCACAAGAACCTTATCCATATGCTCCACCTCATGCTTTTTCTCCTCCTCATCCATCTTATTTACATCCATTACCTCCACCTGCTCATGCTGCA
1801 CCACCACCACCACAAACAGATGATGATAGACATGCAGCTTTATTAGCTAGAAAGGAAAGAATGAGAGAAGAGCAAGAACAAATTAGAAGAGAGGAGGAAG
1901 CTTTAGCTTCTGGTGGTGGTGGTGGTTCTGGTGGTGGTCAATAA
```

***C. ferigula* PYCC4410 *HD2* synthetic gene sequence**

```
   1 ATGCCGGATGATACTGCTCTTCTGCAGAATGTTTTGAAGCTTGCACAGGAGTTAGGTCAGTCTGCTGGAGTCCCGCTCAGTACAGGAAGACCACTTACCT
 101 TACCGGAGTACCTCCCGCTGGATCTCCCACCTCCCCCCACCTTGTCGAGATATCTAGAGTCGATTGGGATTTCACCGGCTTTGCAAGCAGCTCTGCAACT
 201 TGCATTCGAAAAAAGAATCCGAACATTTGCCATATCAACTCAACAATTGTATCAGCGATCGTCTGGGGGAGTGAGTGCACCATTGGGTGTCTTGGAGGAG
 301 GTCAATGGGTCTAGGGGCTACGCGGCTAGATTGTTCCGTGACTTCCGTGCTCAAGTGATAGCCCACTTTGTAACCGAAGTTGCCAAATTGCAAGCCATGG
 401 TTTTAAGCAAGGCAAGGGACCATGTACTGAAGGCTGGATCCACTAAACCGCCTCCCCAGTTCACTAAAGCTCACCCATTGAGCAGTCATCCTCCCACTAG
 501 CGCTATAGAAACACTGCGGAAGCTGTACTTGTTAAATACTTACCCTAACCCTGCAGAAATACGTTTGATAGCTAAAAAAATCCAGATGGATTACAAACAG
 601 GTGAGGGTCTGGTTTCAAAACCGTAGGAACAGAAAAGCTGTCTCCGCACGCGGACTAAAGGAAGAAGTAAGGATCGCACAGGCTTCCGGCATCAAATTAC
 701 CGTCCACGCACAAGCGTGAGTTGAGAAAACTTGAGACAGCCGCTGCAAAGCAAACTAGGAAGAAGGATGGCGAGAGAAGACGCAGAGGAGGCGTAGTCGT
 801 CACAGCTCAGGATGTACAAGATGAAGACAAAGAAGGCATGCATGTGGACGATGCCGGCATCGCTCCTCCGACAGCCAAACATAGCGCTCTAGACACGGTA
 901 TCCTTCAATTATGGGGATGTGTCAATTCTTGGTTATGGCAGACCACCTCCCGTTTATTTCGGAGCGGGAAGTTCAGAGACATCGCCAGCACCCCACAGTG
1001 CTAGTGCTGCTAGCTCCTCTCTATCGTTGTCTGGTCAACCCCCTCCCCCATCATCCTTAGTGCCCAGTGGTTCTTGGAGCTATGATGCTTCCCCCTCCCA
1101 ATGTTCTCAATCGATGACTATTCCAGATGAACAATGGAATCTTGTTCCAGCTAGACCAGACTACTATCAACAAAGACATTCTGACGGTTCTGTTTTAGTT
1201 CCACCTCCAGCAACGGCACAACCTCATAGAACGACCTCATTCGGTAGCAGCTCAAGTTCATCAGGTCTTTCGGATCTAGATTCCTTGTGGTCAATTGCAA
1301 GTACCGATCCAGCGGCGACTTACTCCTCTTTCACATCAGCTCCTTGTGTTCCTACTGCTTTAGACTTTACCCCTCCTTTGCCTTCTGATGAAAGTACTTT
1401 GGCGGCTGCACATGAAAACCCTCTATTCGAACCACCAGAATATTTATTACAATCTTCAATTCCTGAATTCAGTTTTTCTCCATCTCCTCCACCAGCCCTA
1501 AATCCAGCATGTGCCTCTAATCTAGGTTTTTCTGCAGATGATTTTAGAGCCGTTTTAAACGCCGATCCTTTTTCAGACTCTTCTGCCGACGCGTTAGCGC
1601 AAGCTGACTCTAACGGTTTTTTTTGGAATTGCTCAGGTGGTGCGGGTGCAGACGTTTTAGAATTATCAGCCGAAATTGATCAAGTTTTAAGAGCATTTAC
1701 ACCAGAATTTTTAGGTGCTCCAGGTGCCGAAGGTGAAGCATTTGATCCATATGATTGGGGTATTCCAGCCCCAGCAGATACAACCTATCCAGAACCAGTT
1801 TGGTAA
```

Fig. S4. DNA sequences of the designed synthetic *HD1* and *HD2* genes of *C. ferigula* PYCC 5628 and PYCC 4410, respectively. Sequences correspond to the coding DNA sequences of the *HD1* and *HD2* genes of PYCC 5628 and PYCC 4410, respectively, optimized for the codon usage of *S. cerevisiae*.

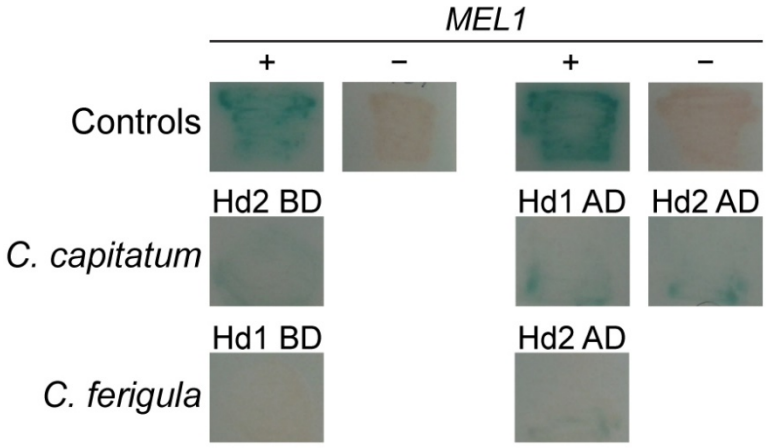

Fig. S5 Activation of the reporter genes in the Yeast Two-Hybrid Assay by the individual fusion proteins. This control consists in assessing activation of reporter genes in haploid transformants carrying each of the fusion proteins to be tested. Absence of this so-called autoactivation shows that activation of reporter genes in diploid strains requires the presence of both interacting partners. Controls are the same as in Figure 4. AD, activation domain of Gal4; BD, DNA binding domain of Gal4.